

EXPERIMENTAL ANALYSIS OF ASH AND MINERAL SOURCES FOR ANCIENT GLASS
USING OXYGEN ISOTOPES

By

LORI ELIZABETH DEMOSTHENES

(Under the Direction of Samuel E. Swanson)

ABSTRACT

Early glasses, known since c. 2500 BC (Henderson 2013), used plants (ash) and minerals (natron) as sources for alkali to flux silica. Mineral and plant alkali samples from the Corning Museum of Glass were combined with quartz from Spruce Pine, North Carolina in a series of experiments to make glass. Oxygen isotope compositions of alkali samples and quartz were measured at various stages of the glass-making process. Initial differences of oxygen isotope compositions gradually converge with higher heating temperatures. Glasses produced with mineral and plant alkali sources could not be distinguished based on oxygen isotope compositions. Therefore, oxygen isotope compositions are not useful in identifying the alkali source used in glass-making.

Key words: natron, glass, plant ash, oxygen isotopes

EXPERIMENTAL ANALYSIS OF ASH AND MINERAL SOURCES FOR ANCIENT GLASS
USING OXYGEN ISOTOPES

By

LORI ELIZABETH DEMOSTHENES

B.A., Appalachian State University, 2011

A Thesis Submitted to the Graduate Faculty of The University of Georgia in Partial Fulfillment
of the Requirements for the Degree

MASTER OF SCIENCE

ATHENS, GEORGIA

2013

© 2013

Lori Elizabeth Demosthenes

All Rights Reserved

EXPERIMENTAL ANALYSIS OF ASH AND MINERAL SOURCES FOR ANCIENT GLASS
USING OXYGEN ISOTOPES

By

LORI ELIZABETH DEMOSTHENES

Major Professor: Samuel E. Swanson

Committee: Doug Crowe
Paul Schroeder

Electronic Version Approved:

Maureen Grasso
Dean of the Graduate School
The University of Georgia
December 2013

TABLE OF CONTENTS

	Page
LIST OF TABLES.....	vi
LIST OF FIGURES.....	vii
INTRODUCTION.....	1
PREVIOUS STUDIES.....	3
<i>Early History of Glass-making</i>	3
<i>The Glass-making Process</i>	3
<i>Melting of Quartz</i>	4
<i>Plant Ash Flux</i>	4
<i>Natron Flux</i>	4
<i>Classification of Ancient Glasses</i>	5
METHODS.....	8
<i>Raw Materials</i>	8
<i>Glass-making Experiments</i>	24
<i>Electron Microprobe Analysis</i>	29
<i>Oxygen Isotope Analysis</i>	31
RESULTS.....	33
<i>Glass-making Experiments</i>	33
<i>Glass Compositions</i>	34
<i>Oxygen Isotope Analysis: Plants and Ashes</i>	38

<i>Oxygen Isotope Analysis: Mineral Alkalis</i>	41
DISCUSSION	42
<i>Composition of Raw Materials</i>	42
<i>Composition of Glasses</i>	45
<i>Oxygen Isotopes</i>	47
CONCLUSIONS	50
REFERENCES	52

LIST OF TABLES

	Page
Table 1: Chemical analyses of raw materials (from Brill 1999)	9
Table 2: Oxide compositions for mineral samples based on ICP/MS	11
Table 3: Descriptions of all glass experiments	26
Table 4: Descriptions of successful glass experiments.....	28
Table 5: EMPA results for successful glass experiments	31
Table 6: Comparison of Corning Museum Glass Standards	34
Table 7: EMPA Results of Glasses 6 and 7 from this study and Stapleton (2003)	35
Table 8: Comparison of expected vs. measured glass compositions.....	36
Table 9: Oxygen isotope ratios for halophytic plants.....	38
Table 10: Oxygen isotope ratios of raw materials, fritted alkalis and glasses.....	40
Table 11: Oxygen isotope ratios for plants, ashes, fritted ashes, and plant ash glasses	41
Table 12: Oxygen isotope ratios for the mineral alkali, heated mineral, and glasses.....	41
Table 13: Theoretical and Measured $\delta^{18}\text{O}$ ratios for plant ash glasses.....	48

LIST OF FIGURES

	Page
Figure 1: Compositional fields of soda glasses	6
Figure 2: Oxygen isotope data for ancient glasses (from Brill et al. 1999).....	7
Figure 3: Petrographic photo of Spruce Pine quartz.....	8
Figure 4: XRD pattern for mineral sample 326.....	12
Figure 5: TGA results for mineral samples 324 and 326.....	13
Figure 6: XRD pattern of Sample 656.....	15
Figure 7: XRD pattern of sample 658.....	16
Figure 8: TGA results for mineral samples 656 and 658.....	18
Figure 9: XRD pattern for WY trona.....	19
Figure 10: Map showing the source locations for various alkalis	20
Figure 11: XRD pattern for plant ash 1330	22
Figure 12: TGA results for plant ashes 1331 and 4417.....	23
Figure 13: SiO ₂ - Na ₂ O phase diagram (after Kracek 1930)	27
Figure 14: Na ₂ O - CaO - SiO ₂ with 5 wt% MgO phase diagram	29

Figure 15: Plot of MgO against K₂O for the experimental glasses38

INTRODUCTION

Archaeological evidence shows that glass has been produced and used in the mid-East since c. 2500 BC (Henderson 2013). Glass was associated with power and prestige. In ancient Egypt, only pharaohs, high priests and nobles owned glass objects (Zerwick 1990). The first glass-making centers were located in centers of religious and political power, likely because in only these areas were skills and technical knowledge able to be maintained (Oppenheim et al. 1970). As the knowledge of glass-making spread, artisans adapted the technology to suit their circumstances, using the raw materials available in their area.

Ancient glasses were made by mixing three basic components: a glass-former (silica), a flux (Na/K-rich material), and a stabilizer (Ca-rich material). Beach sand (quartz and shell fragments) was the usual choice to serve as both the glass-former and stabilizer (Turner 1954, Henderson 1985). However a variety of materials were used to flux glasses, the most common being ash from halophytic (alkali-rich) plants or Na-rich evaporite minerals such as natron ($\text{Na}_2\text{CO}_3 \cdot \text{NaHCO}_3 \cdot 2\text{H}_2\text{O}$) and trona ($\text{Na}_3(\text{CO}_3)(\text{HCO}_3) \cdot 2\text{H}_2\text{O}$).

The raw materials used as a flux varied through both time and space. According to researchers and ancient texts, plant ash was the original flux, which was used until approximately 800 BC (Oppenheim et al. 1970, Lilyquist and Brill 1993, Henderson 2013). From around 800 BC to 800 AD, natron was used as the primary source for alkali to flux, followed by a switch back to plant ash between 800-900 AD (Henderson 2013). It is unclear why these changes took place; suggestions range from depletion of the natron source to a change in climate that resulted in a change in evaporite mineralogy (Silvestri et al, 2010; Shortland et al., 2006).

Chemical analyses of glasses can shed light on the raw materials used to make the glass. Shifts in raw material usage may provide provenance information and evidence for trade of raw materials and/or glass recycling (Henderson 2013). Oxygen isotopes have previously been shown to vary greatly between plant ashes and evaporite minerals (Brill 1970), suggesting that this distinction will persist through the glass-making process and create two isotopically distinct glasses.

This study presents chemical and isotopic data for experimental glasses made using mineral or plant ash alkali sources as the flux. The raw materials were examined by Thermogravimetric (TGA), and X-ray diffraction (XRD) for chemical characterization. Glasses were analyzed by electron-microprobe analysis (EMPA). Oxygen isotope analysis was performed on the raw materials and at each step of the glass-making process to test the hypothesis that isotopic signatures persist through the glass-making process and into the final glasses.

PREVIOUS STUDIES

Early History of Glass-making

Vitreous pottery glazes are considered to be the first glassy materials and were in use long before glass appeared as an independent material (Douglas and Frank 1972). The first glass objects to appear in the archaeological record are small beads that date to at least 2500 BC (Moorey 1999). Glass vessels began to appear in the archaeological record around 1500 BC (Shortland et al., 2006). Vessels require intricate glass-forming techniques and are much more difficult to make than smaller objects. The technology was first developed in western Asia or Mesopotamia and was brought to Egypt during the reign of King Thutmose III (1504-1450 BC) (Douglas and Frank 1972, Zerwick 1990). Thutmose III led a series of conquests into Asia beginning in 1481 BC, and historians suggest that he brought back glass artisans to set up a glass industry in Egypt (Douglas and Frank 1972).

The Glass-making Process

Making glass consists of 5 steps: selection and preparation of the raw materials, mixing and initial heating (fritting) the batch of raw materials, grinding and melting the frit, forming the glass into its final shape, and then annealing the glass objects. Raw materials are gathered and prepared (plants are ashed), and then crushed, mixed, and fritted. In the fritting stage, the raw materials are heated together at sub-solidus temperatures (around 700-800 °C). This temperature is low enough to not induce melting; rather a granular, annealed material is created and referred to as a 'frit' (Henderson 2000a). This step drives off absorbed and structural water and organics components (Henderson 2000b). Then the glass is heated to the melting temperature, around

1100 °C and worked (formed in a mold, coiled around a core) while still malleable. Once the desired shape is achieved, the object is annealed and slowly cooled to relieve the strain created during object formation (Henderson 2000a).

Melting of Quartz

Pure SiO₂ melts at 1700°C at 1 atmosphere. Glassmakers during ancient times did not have the technology to reach such a high temperature, so a flux was added to quartz sand in order to lower the melting point of SiO₂ to a more achievable temperature. Both plant ashes and evaporite minerals (natron or trona) were used to flux quartz.

Plant Ash Flux

The first glasses were made with ashes from plants of the Chenopodiaceae family (Barkoudah and Henderson 2006). The plants grow in arid regions and withstand high levels of alkali in the soil (Henderson 2013). Halophytic plants concentrate alkali salts in their stems and leaves through transpiration. Upon ashing, these plants produce sufficient quantities of sodium carbonate to make them suitable for glass-making (Henderson 2013). The sodium carbonate in the plant ash reacts with the silica component to lower its melting temperature from approximately 1700°C to a more easily achievable 1100 °C (Henderson 2013).

Natron Flux

Natron was introduced as an alkali source around 1000 BC, followed by a transitional period as it began to replace plant ash (Sayre and Smith 1961, Lilyquist and Brill 1996, Henderson 2013). Natron commonly refers to sodium-rich evaporite deposits containing a variety of Na-bearing minerals (including natron). Pliny the Elder, tells of the “Invention” of natron glass on the Levantine coast in Book XXXVI, of his *Naturalis historia*:

“The beach extends for not more than half a mile, but for many years this area (Sidon) was the soul producer of glass. A ship belonging to the trades in soda once called here, so the story goes, and they spread out along the shore to make a meal. There were no stones to support their cook pots so they placed lumps of soda from their ship under them. When these became hot and fused with the sand on the beach streams of an unknown translucent liquid flowed and this was the origin of glass” (in Henderson 2013)

Natron is not only denser than plant ash but also typically contains higher levels of alkali, therefore making it a more efficient flux (Henderson 2013). Wadi Natrun is a group of evaporite lakes in Egypt, located west of the Nile River, that is known natron source that was exploited for glass production during ancient times (Brill 1999, Shortland and Tite, 2000, Henderson 2013). Little is known of other sources of natron. Around 800 AD, the use of natron in glasses began to decline (Shortland et al. 2006). The decline is attributed to either a shortage of the mineral or a change in climate that resulted in a change in the evaporate mineralogy, making the Wadi Natrun salts no longer suitable for glass-making (Sayre and Smith 1961,1967; Henderson 1985, Freestone et al. 2000).

Characterization of Ancient Glasses

Ancient glasses are traditionally classified as either high magnesium glass (HMG) or low magnesium glass (LMG) (Fig. 1). These classifications were first identified by Sayre and Smith (1961) using emission spectroscopy, and then later reanalyzed with Neutron Activation Analysis (NAA) (Sayre and Smith 1974). Figure 1 is taken from Lilyquist and Brill (1996) and shows the compositional fields for glasses made unequivocally from either plant ash or natron.

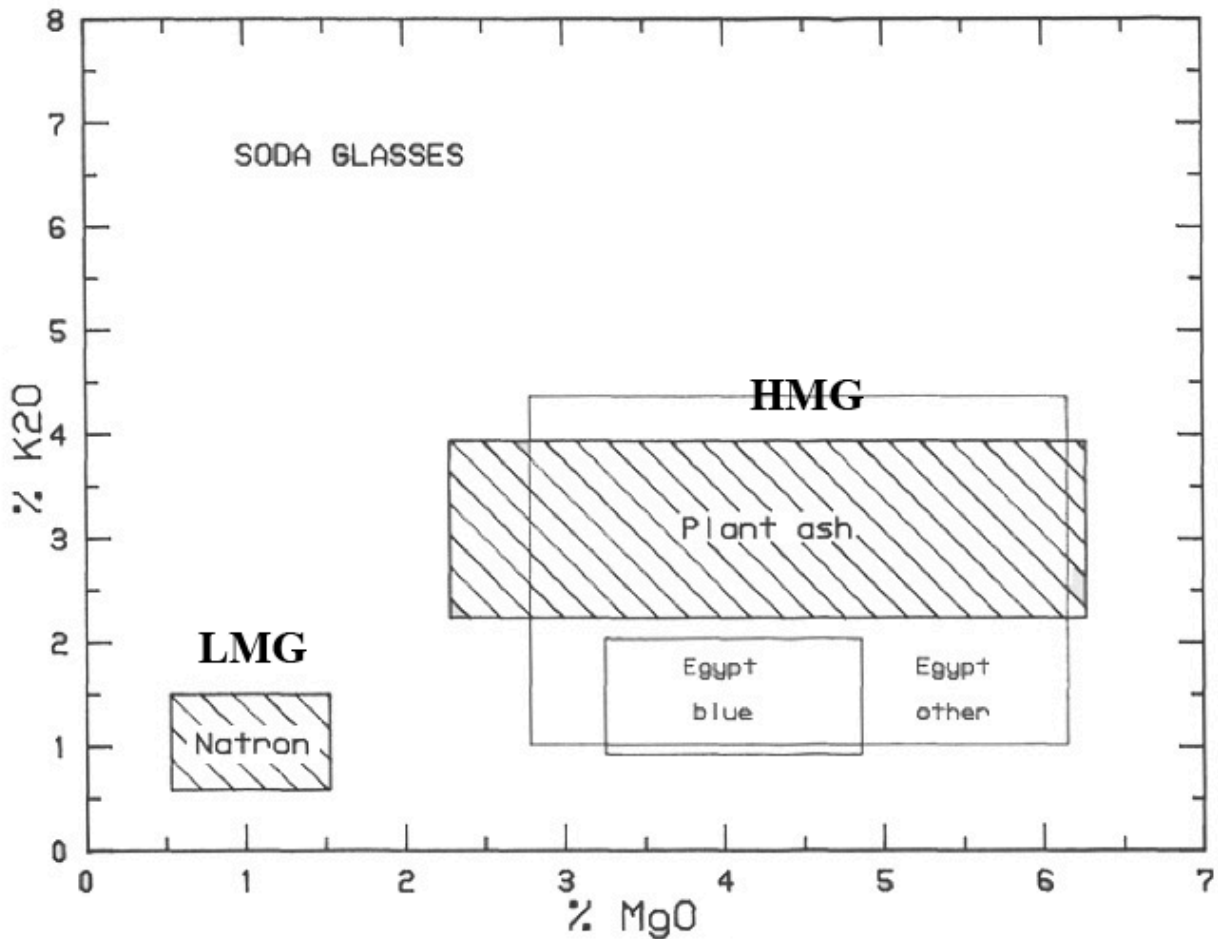


Figure 1. Compositional fields of soda glasses based on K_2O and MgO content (after Lilyquist and Brill 1996). LMG = low magnesia glass, HMG = high magnesia glass. Egyptian blue glasses (made with natron and added cobalt alum) and other Egyptian glasses are also plotted.

The HMG glasses are typical of those made with plant ashes, while the LMG glasses are characteristic of natron glasses (Sayre and Smith 1961, Sayre 1974, Henderson 1988, Lilyquist and Brill 1996). However, many glasses cannot be characterized based on these criteria alone, as their MgO and K_2O contents fall outside the accepted values for HMG or LMG glasses (Stapleton 2003). In some cases, these glasses can be reconciled with the natron or ash fields by considering other components added to the glass (for example, a cobalt-bearing alum produced the blue glasses in Figure 1, but also added another 3 weight percent MgO to the glass).

A reliable method for identifying the source of the alkali flux used to make ancient glasses has yet to be established. Brill (1970) and Brill et al. (1999) report oxygen isotope analyses of ancient glasses and potential glass raw materials (quartz, natron, limestone and shells) and showed an overlap of the raw materials and ancient glasses (Fig. 2).

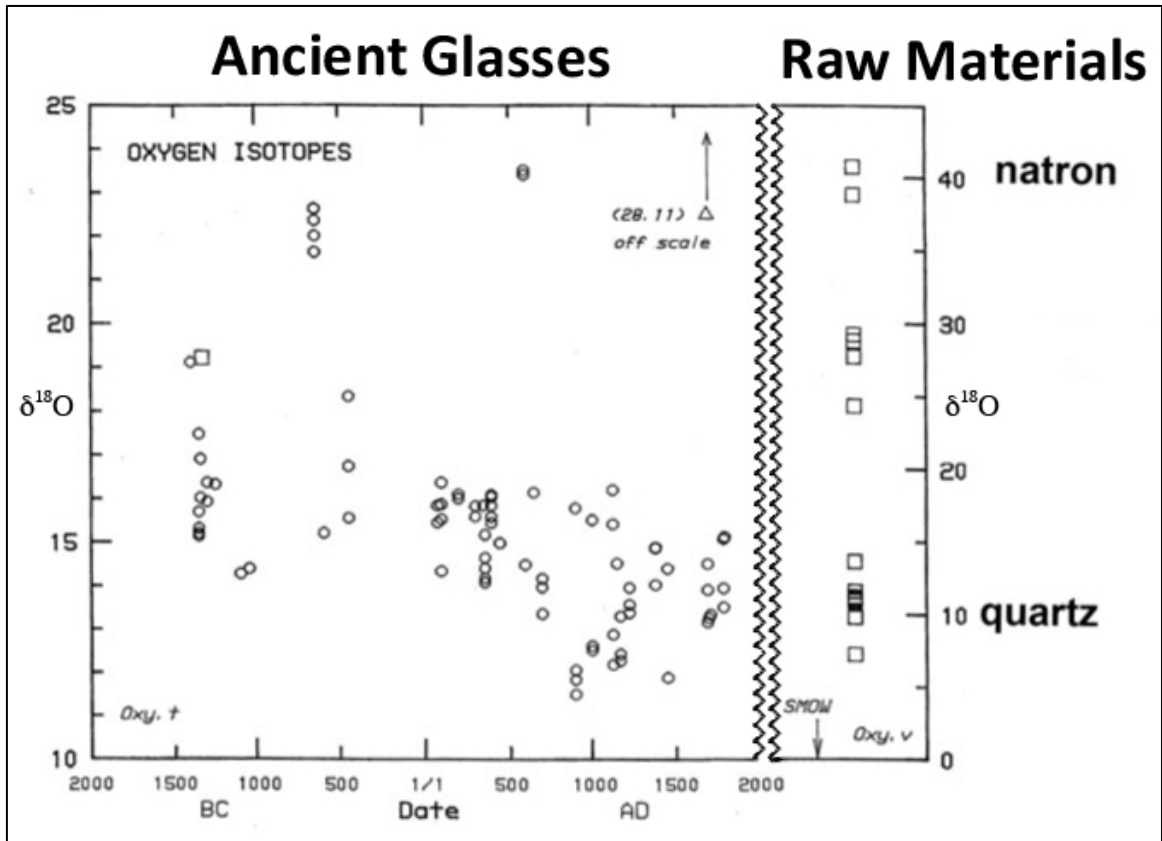


Figure 2. Oxygen isotope data for ancient glasses arranged by dates and potential raw materials (from Brill et al. 1999). Note the difference in scales between glasses and raw materials

Based on these results, workers continue to examine the role of oxygen isotopes in the study of ancient glasses (e.g. Henderson et al. 2005, Henderson and Barkoudah 2009, Silvestri et al. 2010). Chemical analysis alone has been unable to determine source and type of raw soda materials used to make ancient glasses.

METHODS

Raw Materials

Quartz

Glasses were made using quartz from Spruce Pine, North Carolina. The Spruce Pine quartz is a first-stage separate made during granite processing to produce an ultra pure quartz product. The quartz contains rare grains of garnet and epidote (Stapleton 2003). A grain mount of the quartz that was examined under the petrographic microscope exhibited no garnet or epidote grains, this study assumes the Spruce Pine quartz is essentially pure SiO₂ (Fig. 3).

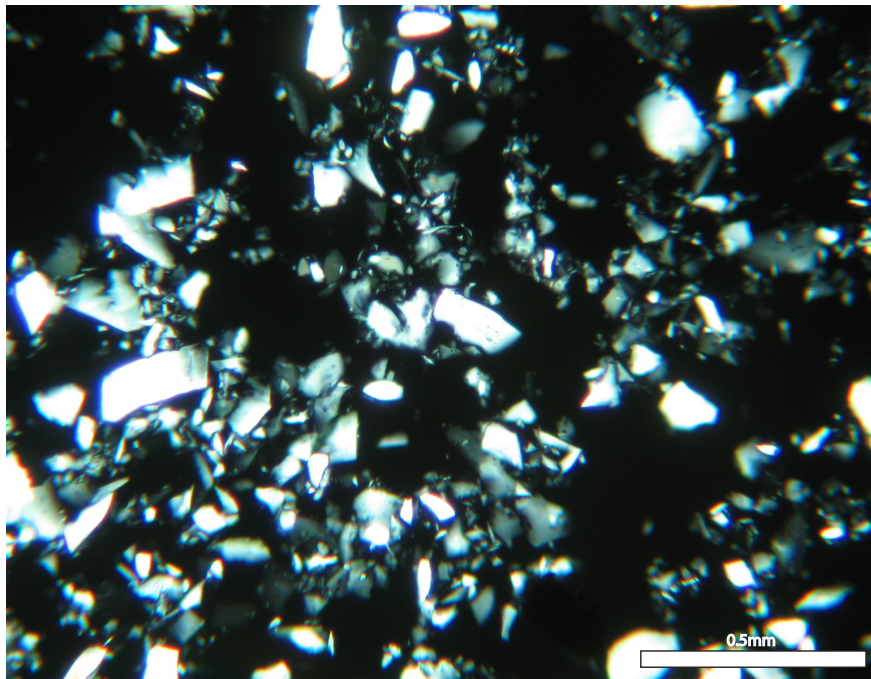


Figure 3. Photomicrograph of Spruce Pine quartz under XPL

Mineral Alkali Sources

Mineral alkali sources catalogued by Brill (1999) and curated at the Corning Museum of Glass (CMOG), in Corning, New York were used in some of the glass-making experiments (Tables 1a and 2).

Table 1a. Chemical Analyses of mineral alkalis from CMOG catalog done at UGA (from Brill 1999).

CMOG alk #	323	324	326	655	656	658
source		Wadi Natrun			Egyptian tomb	
SiO ₂	“minor”	“major”	0.05	~0.5		~2.0
TiO ₂	0.00X	0.X		0.005		.2
Al ₂ O ₃	0.X	“minor”	0.005	0.10		0.47
Fe ₂ O ₃	0.00X	“minor”	0.003	0.14		0.26
MnO	0.000X	0.00X hi	0.001	0.001		0.0005
MgO	0.0X	0.X	0.005	0.38		0.46
CaO	0.X	“minor”	0.02	0.3		0.42
Na ₂ O	“major”	“major”	“major”	50.5		41.6
K ₂ O	0.X	0.X	0.02	.55		0.58
SO ₃				7.1		6.68
Cl				38.88		9.52
CO ₂				8.0		8.5
Total				105.96		68.72

Table 1a. Analyses done by Brill (1999) were done over a 40 year periods with various analytical methods including: Flame photometry, optical emission spectrometry, atomic absorption, Inductively coupled plasma (ICP/MS), microprobe, and X-ray fluorescence)

Table 1b. Chemical analysis of plant sample 1380 (from Brill 1999).

CMOG alk #	1380*
description	Chinan plant
source location	Syria
SiO ₂	0
TiO ₂	0.05
Al ₂ O ₃	0.72
Fe ₂ O ₃	0
MnO	0.01
MgO	6.04
CaO	9.54
Na ₂ O	31.3
K ₂ O	5.23
SO ₃	8.10
Cl	15.0
CO ₂	28.2
Total	105.29

*only plant sample analysis from Brill (1999). All other analyses are for plant ashes

Table 1c. Chemical analyses of ash samples from Brill (1999)

CMOG alk #	650	1324	1326	1330	1331	1381
Description	ash from 650 plant	ash from 1324 plant	ash from 1326 plant	<i>Tezab</i>	<i>Ishghar</i>	<i>keli</i>
Source	Turkey	Iraq	Iraq	Afghanistan	Afghanistan	Syria
SiO₂	"minor"	"minor"				2
TiO₂	0.80	0.80	0.02		0.5	0.005
Al₂O₃	5.90	4.89	0.45	0.56	1.14	1.82
Fe₂O₃	3.79	3.52	0.33	0.33	0.39	
MnO	0.02	0.05	0.02		0.05	0.005
MgO	6.25	8.00	12.2	13.3	8.75	11.2
CaO	12.2	13.8	4.67	10.8	7.30	21.2
Na₂O	14.2	25.5	42.5	21.3	35.5	24.0
K₂O	3.98	4.96	7.01	17.2	4.59	15.3
SO₃	3.64	1.73	2.16	1.07	4.74	2.16
Cl	4.24	1.93	6.10	3.81	9.46	3.41
CO₂	1.3	8.6	26.4	19.8	23.0	29.0
Total	57.4	74.86	102.91	88.17	95.98	111.05

Samples 323, 324 and 326 were collected from Wadi el Natrun, Egypt in the fall of 1962 by Robert Brill and Z. Hanna (Brill 1999). This area is a known source for natron for glass-making according to ancient texts by Pliny the Elder (23 B.C.-A.D. 79) (Henderson 2013). Cations in samples 323, 324 and 326 were analyzed by ICP/MS at the University of Georgia in the Center for Applied Isotope Studies in 2003. The analyses (Table 2), show all three samples are very high in Na₂O (~99%).

Sample 326 was analyzed by XRD. The pattern is shown in Figure 4. The XRD pattern shows a very intense peak for halite and minor thenardite (Na₂SO₄/ Na₂O·SO₃) peaks (fig 4). TGA was performed on samples 324 and 326, and the results are shown in Figure 5. Sample 324 (Fig. 5a) has a small peak in the TGA curve just below 200°C related to the loss of absorbed and structural water. Carbonate minerals decompose in the range of 850°C. Sample 324 has three distinct TGA peaks above 800°C related to the breakdown of three different phases. The peak at 860°C is probably related to the breakdown of a carbonate phase. The peak slightly above 860°C may be related to the melting of sodium sulfate (thenardite, melting point 884°C)

and halite. Sample 326 (Fig. 5b) has a single peak on the TGA curve at 840°C related to the melting of halite.

Table 2. Normalized Oxide Compositions based on ICP/MS analysis for modern Wadi Natrun mineral samples

CMOG alk #	323	324	326
Oxide wt %			
SiO ₂	0.01	0.28	0.01
Al ₂ O ₃	0.01	0.16	0.01
FeO*	<0.01	0.04	<0.01
MnO	<0.01	<0.01	0.00
MgO	0.02	0.14	<0.01
CaO	0.07	0.91	0.02
Na ₂ O	99.81	98.18	99.93
K ₂ O	0.05	0.15	0.02
P ₂ O ₅	0.02	0.13	0.01
Total	99.99	99.99	100.00

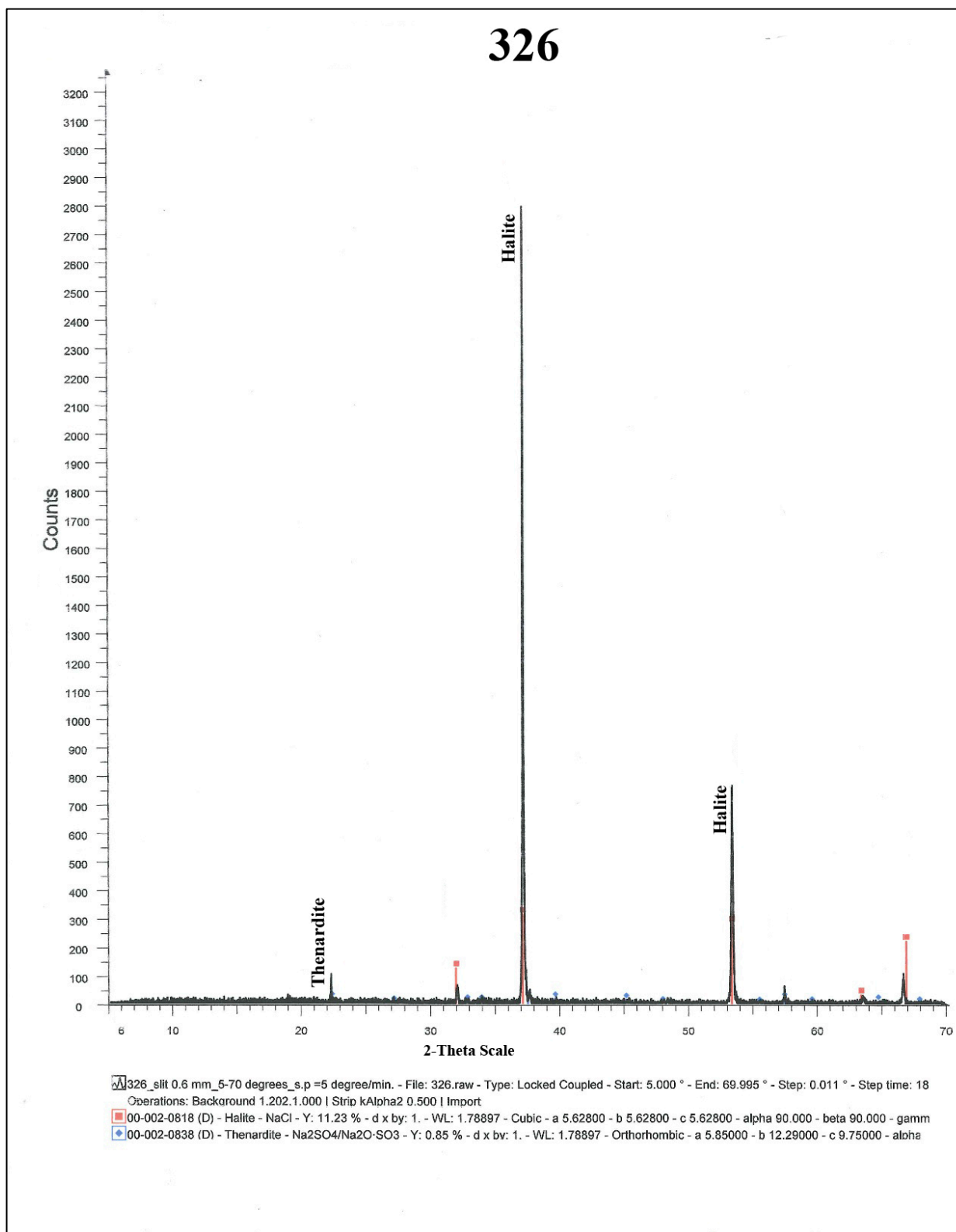


Figure 4. XRD pattern of sample 326. Red square indicates halite, and blue diamond indicates thenardite.

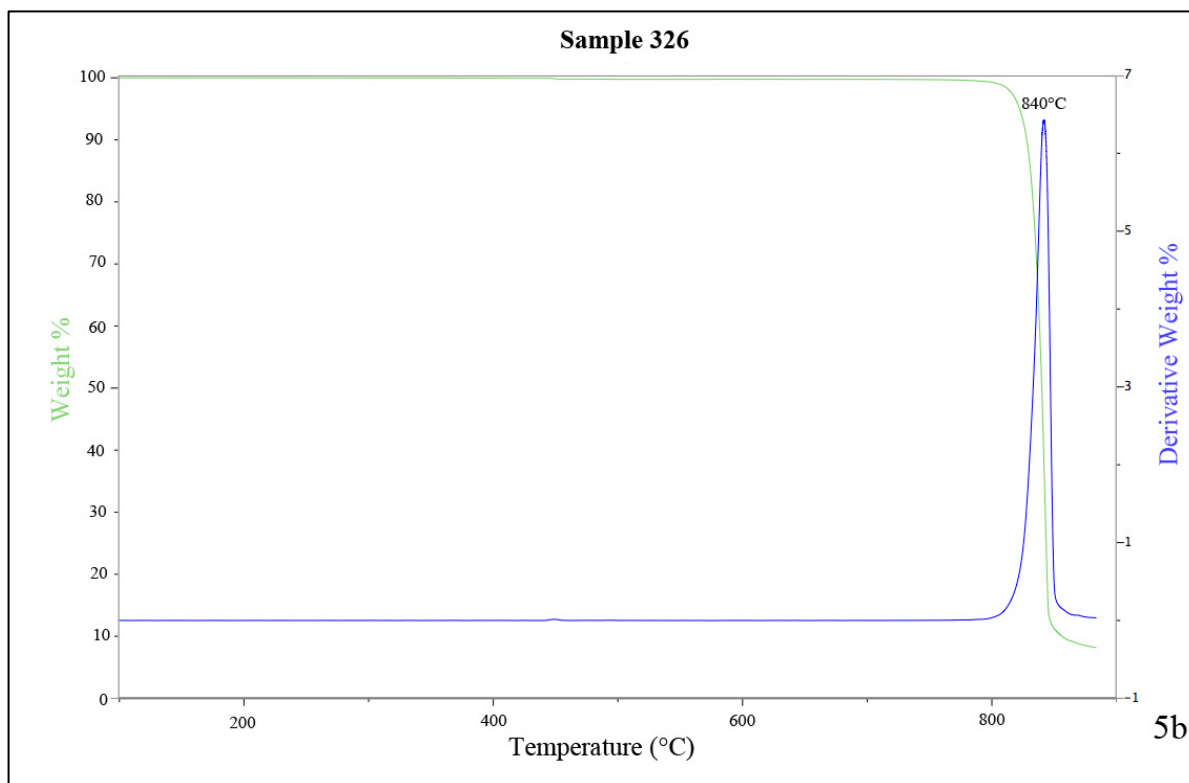
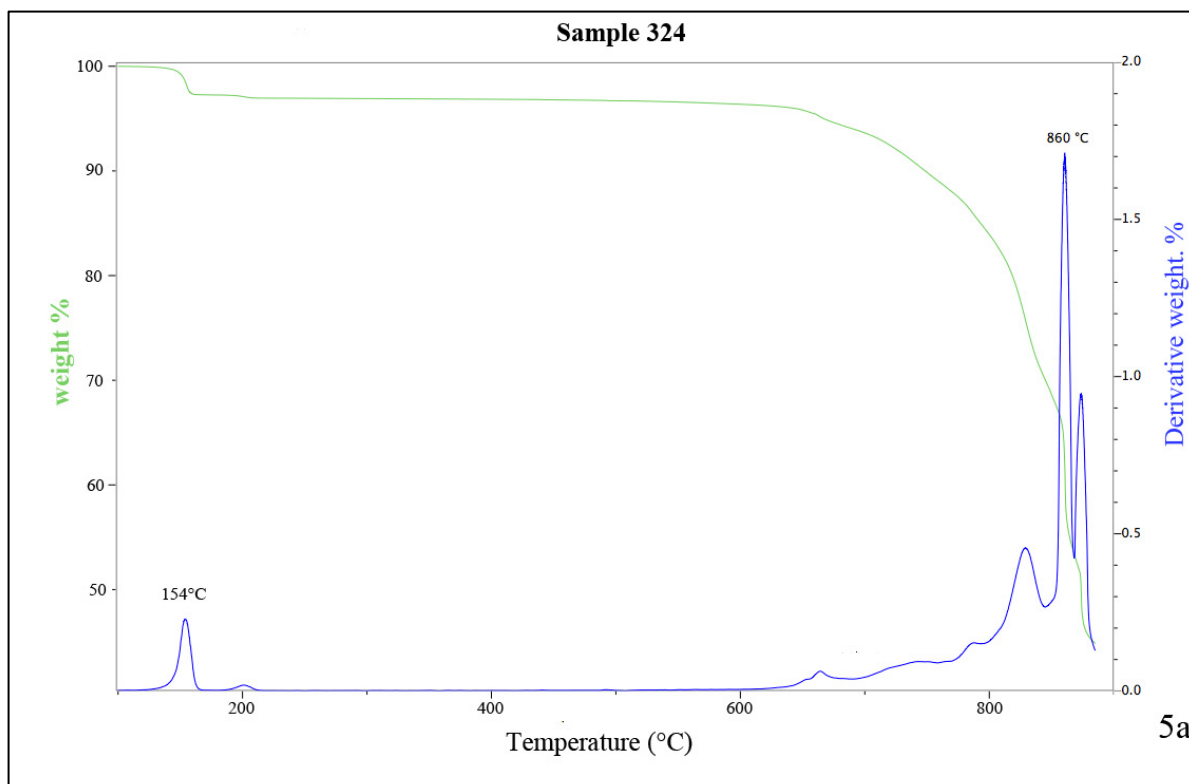


Figure 5. TGA results from mineral alkali samples 324 and 326.

Samples 655, 656 and 658 were taken from caches in the tomb of King Tutankhamen and are assumed to have been collected from Wadi el Natrun during late 13th century BC (Brill 1999). Compositions of the tomb mineral alkali sources are given in Table 1a. The chemical analyses done by Brill (1999) show that the tomb samples are predominately composed of sodium chlorides, sulfates, and carbonates. The chemical analysis of the mineral alkali sample 658 (Table 1a) done by Brill (1999) has very low total, about 69%. Brill attributes the low totals to anions that were not included in the analyses (Brill, 1999).

The XRD patterns show that the samples are made primarily of halite with minor concentrations of other evaporite minerals (Figs. 6 and 7). Halite is the major component of sample 656 with, in order of abundance, minor amounts of trona ($\text{Na}_3(\text{CO}_3)(\text{HCO}_3)\cdot 2\text{H}_2\text{O}$), thermonatrite ($\text{Na}_2\text{CO}_3\cdot\text{H}_2\text{O}$), pirssonite ($\text{Na}_2\text{Ca}(\text{CO}_3)_2\cdot 2\text{H}_2\text{O}$), and mirabilite ($\text{Na}_2\text{SO}_4\cdot 10\text{H}_2\text{O}$) (Fig. 6). Sample 658 is also mostly halite with minor amounts of trona, nahcolite (NaHCO_3), and thenardite (Na_2SO_4) (Fig. 7).

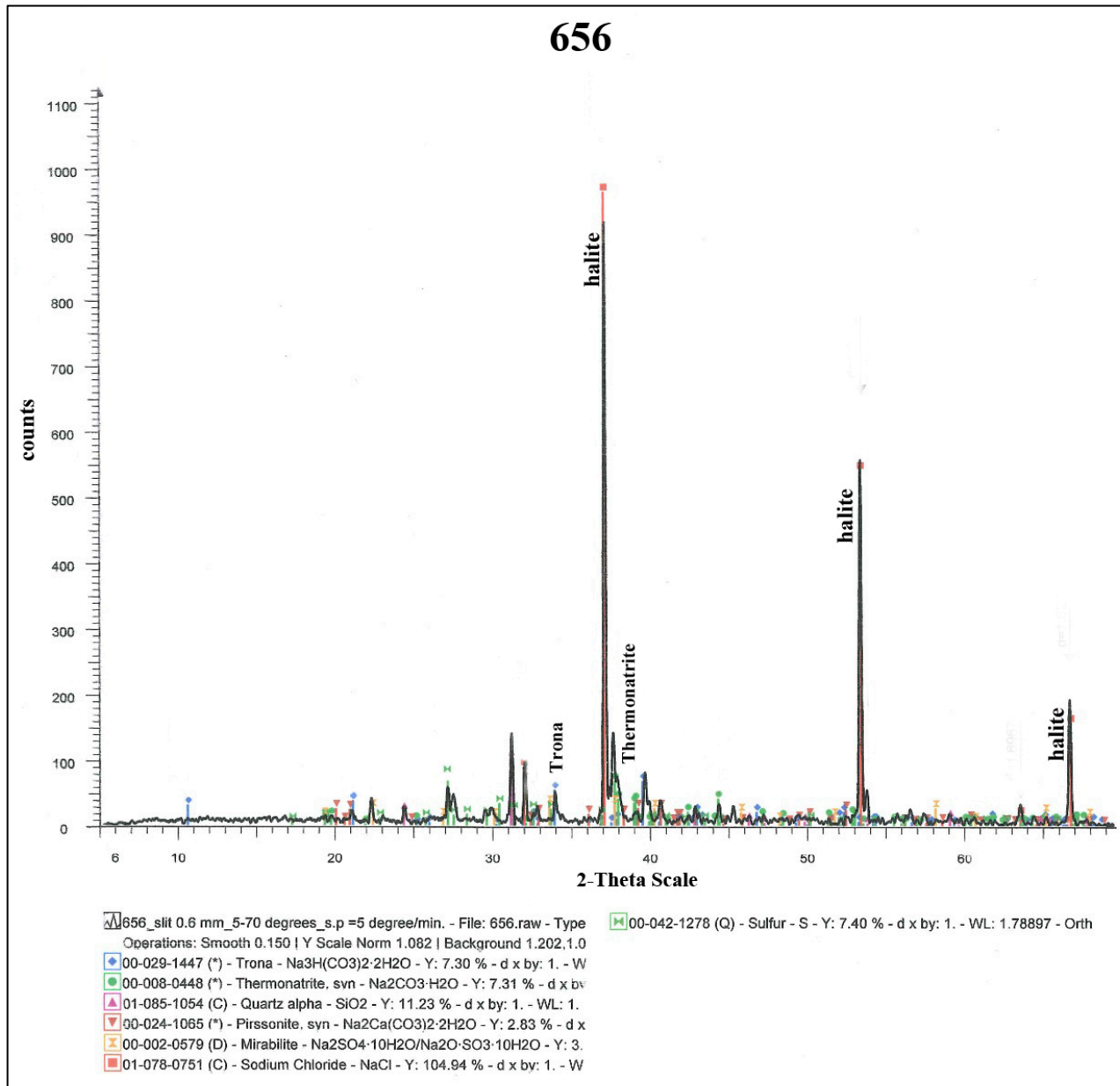


Figure 6. XRD pattern of Sample 656. Major peaks are labeled (halite). Minor peaks are identified by color, and phases are given in the key.

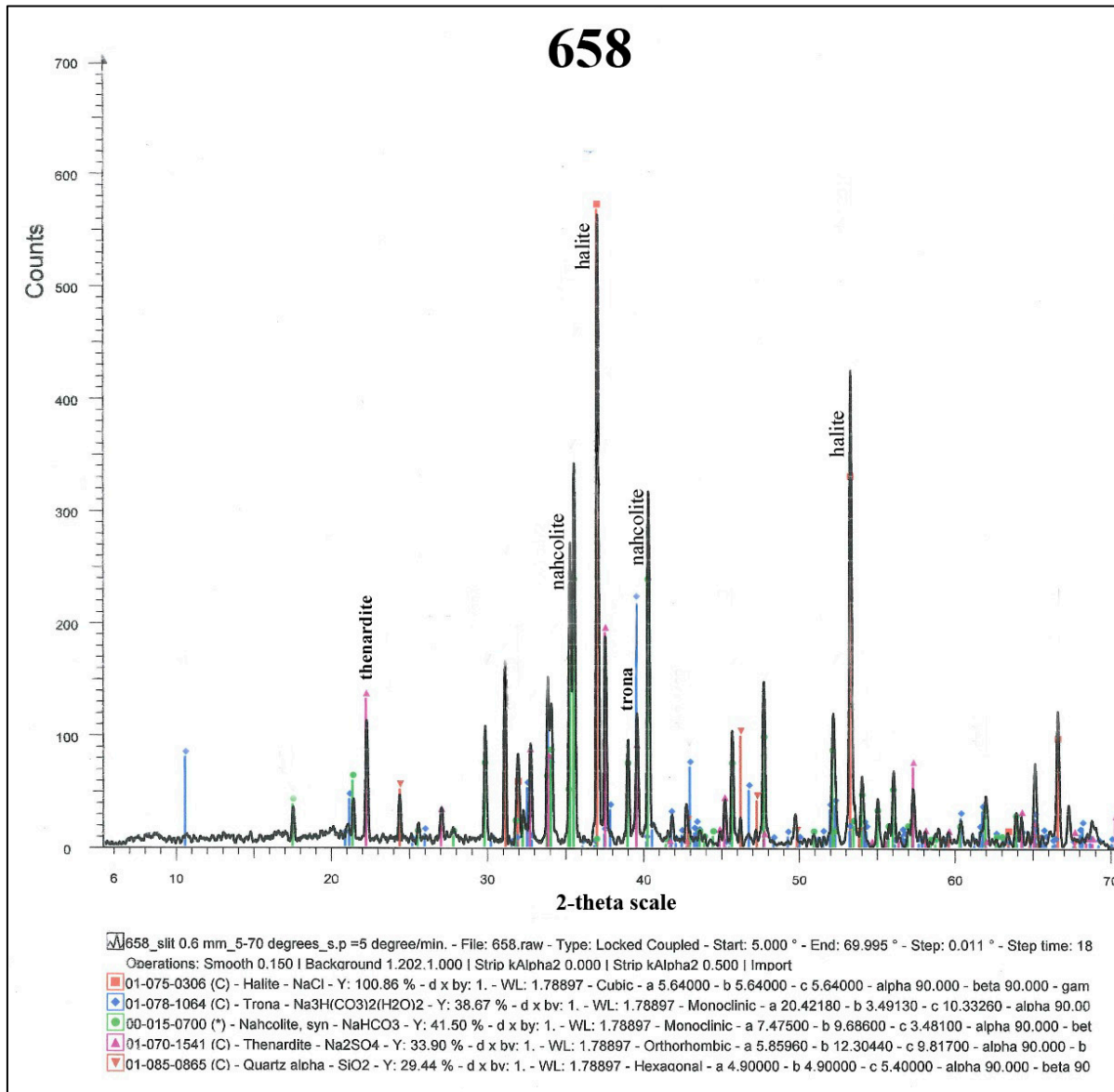


Figure 7. XRD pattern of sample 658, shows major components are halite and nahcolite.

The TGA results (Figs. 8a & 8b) show little change in sample 656 until just above 850°C when a peak indicates the decomposition of a carbonate phase. Sample 658 has a large peak just below 200°C that is related to water loss. The low total for the chemical analysis of sample 658 (Table 1a) is, thus, related to water. Sample 658 shows a slight loss, beginning at 800°C. The lack of well-defined peaks on the TGA curve for sample 658 (Fig. 8b) indicates carbonate phases are not present in appreciable quantities. Despite the identification of trona and nahcolite in the XRD

analysis, this material has not been a successful flux in glass-making experiments. The gradual increase in the TGA curve, terminated at 886°C, may be related to melting of sodium sulfate.

A series of glass experiments used trona from Solvay Minerals, in Green River, Wyoming as the alkali component. The Wyoming trona was selected as a proxy for the ancient mineral alkali raw materials. Trona was referred to as natron by Pliny, and occurs at the modern Wadi el Natrun lakes (Shortland 2004). Therefore the WY trona is an appropriate proxy for the raw materials mined at Wadi el Natrun during ancient times. The WY trona is about 90-93.5% pure trona with up to 10% H₂O-insolubles (clay, quartz, etc.). The XRD pattern of the WY trona showed it to be a rather pure trona, containing no other detectable phases (Fig. 9).

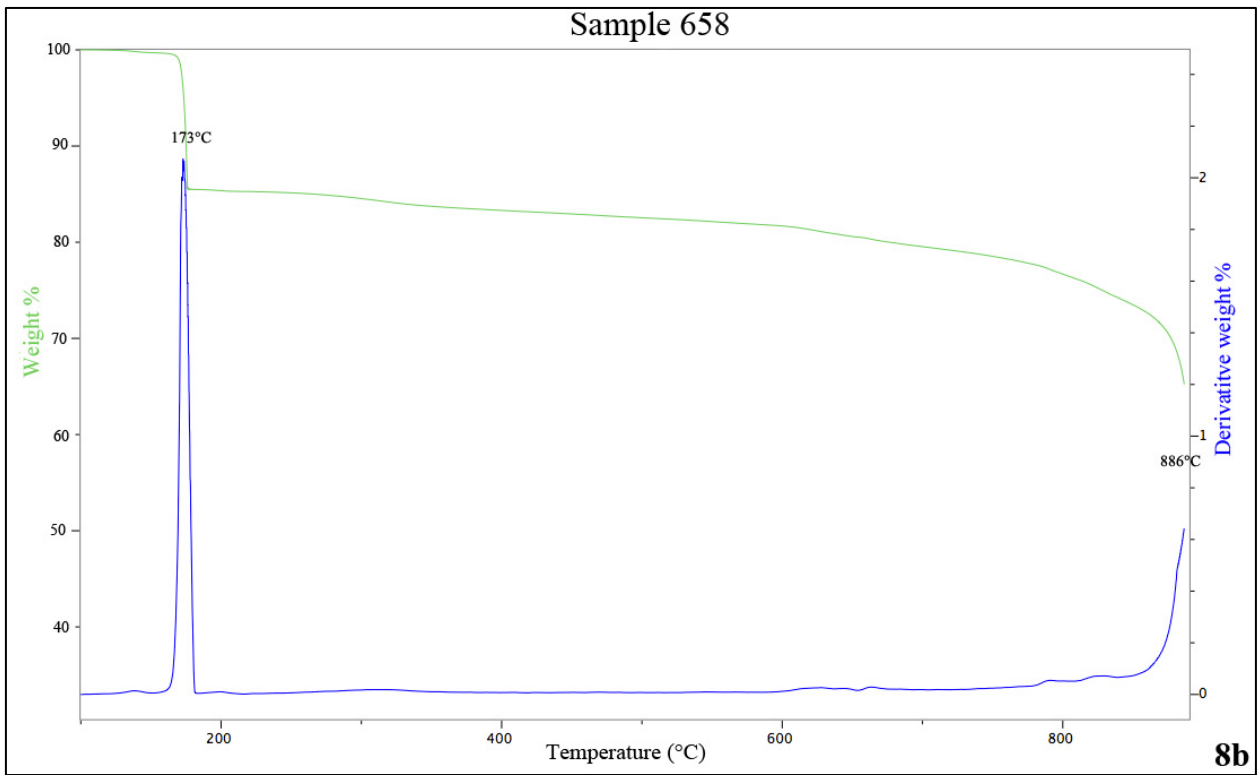
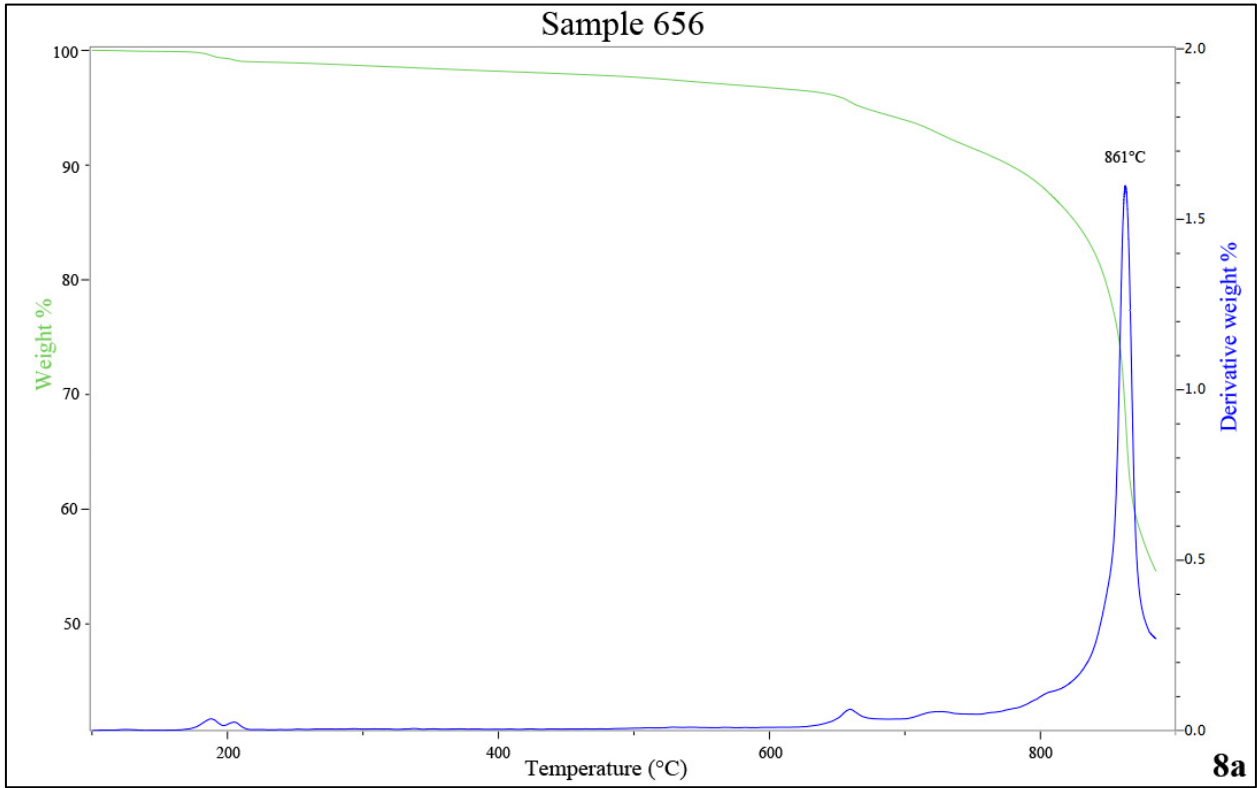


Figure 8. TGA results for the evaporite minerals taken from the tomb of King Tutankhamen.

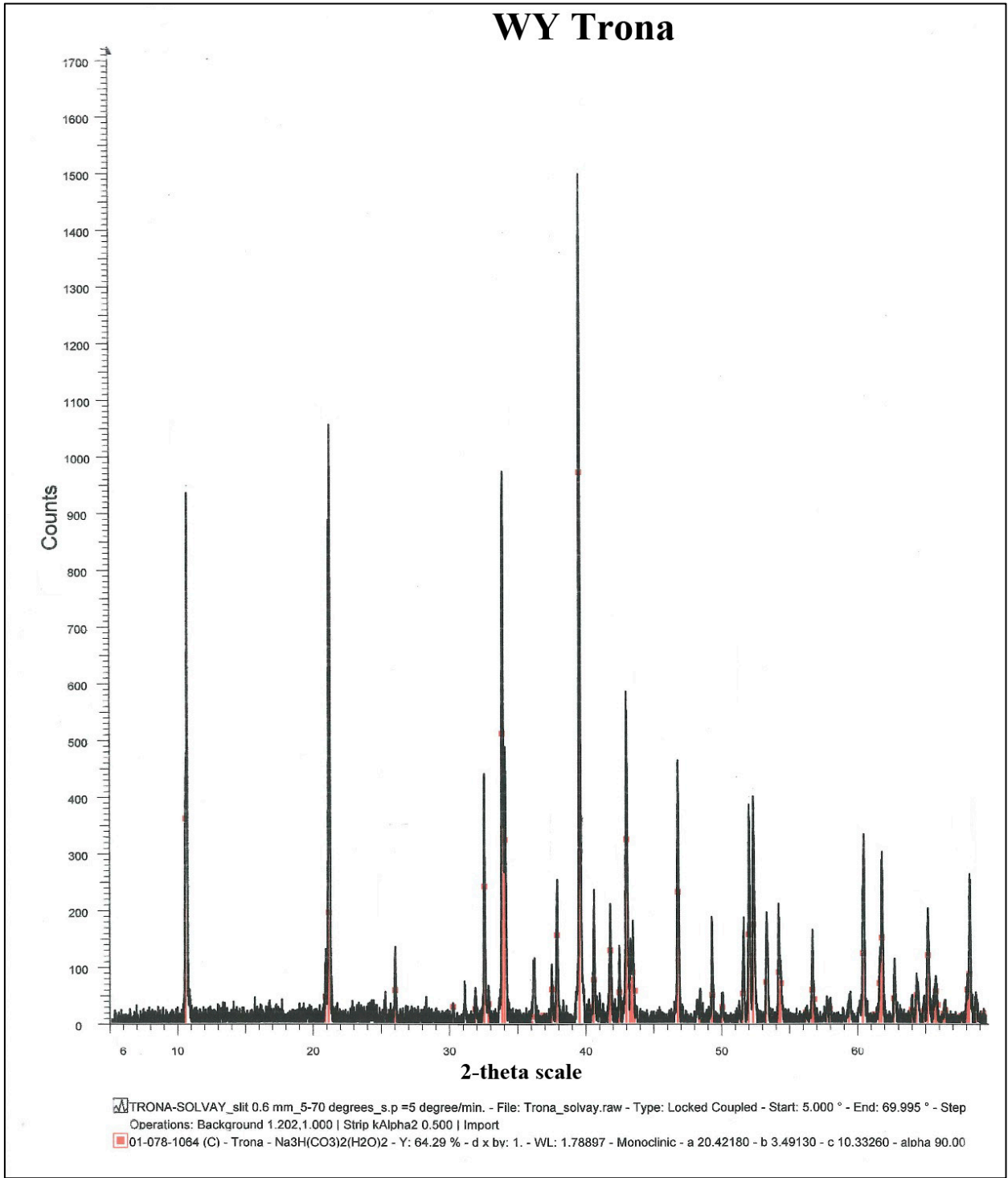


Figure 9. XRD pattern for WY trona. All peaks correspond to trona structure.

Plants alkali sources

Plant alkali sources catalogued by Brill (1999) and curated at the CMOG were used in some of the glass-making experiments. Table 1b lists the plants used in this study and chemical analyses (if available) from Brill (1999). The plant samples were taken from various locations in the Mediterranean region (Fig. 10). Plant samples 650 and 651 are from a halophytic shrub from Turkey. Sample 650 is from the stems, and 651 is the fluffy leaf material shaken loose from the twigs (Brill 1999).

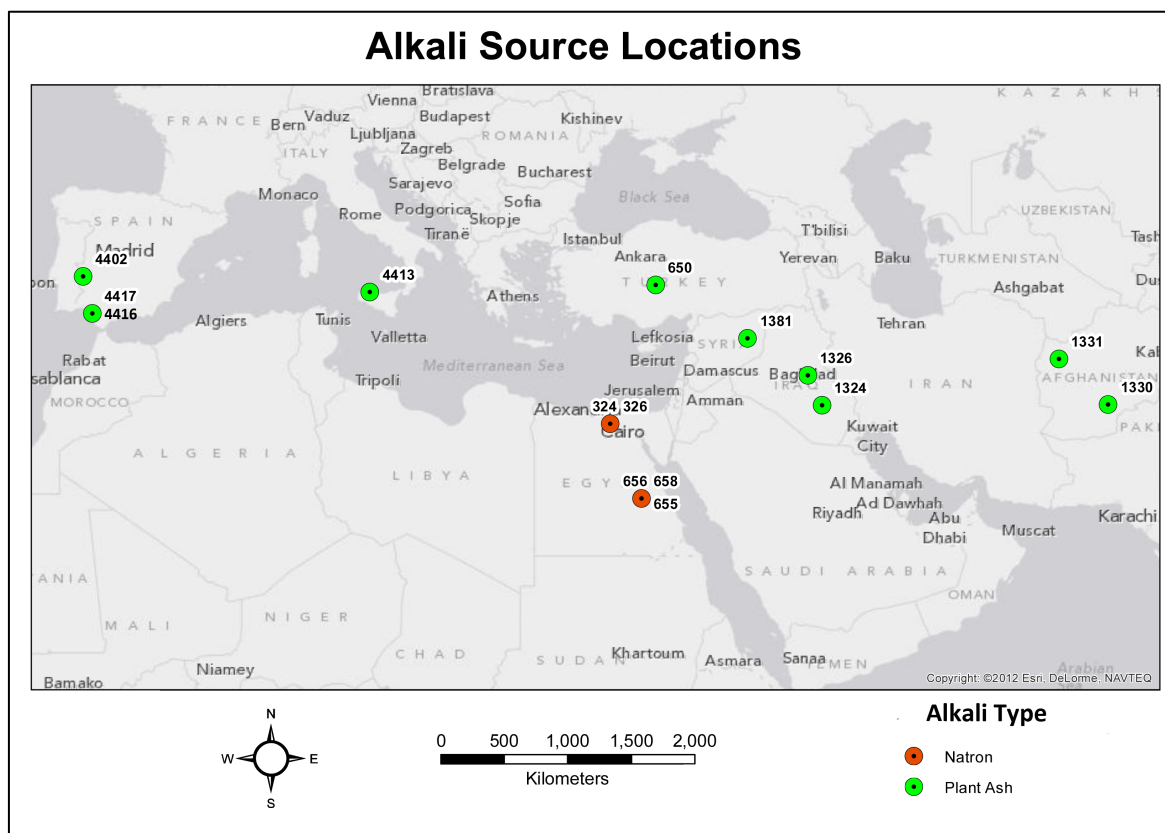


Figure 10. Map showing sources of alkali samples used in glass experiments (map created by Thomas R. Jordan at UGA CRMS)

Some of the CMOG plant samples have both plant and corresponding ash samples, while others are only ashes. Brill (1999) refers to some of the ashes as *tezab*, *keli*, and *Ishghar* (Table 10c). *Tezab* is a plant ash in Afghanistan that is used for soap-making and washing clothes (Brill

1999). *Keli* is a term given for the ash of the *Chinan* plant that grows in the deserts of Syria, which is commonly used in soap and glassmaking (Turner 1954, Brill 1999). *Ishghar* is a term given to plant ash in Afghanistan that is used in glass-making (Brill 1999). Some of the ashes were created at the CMOG lab. Samples 1324, a desert plant from Jezaziyat, Iraq; 1326 “Baghdad souq” a chinan plant used for washing clothes; and 4413, charred stems and debris of *Salsola kali*, collected in Palermo, Sicily; were “slowly burned and then calcined, usually between 700°- 900°C for 1-4 hours” (Brill 1999). The ash samples 1330, chunks of tezeb from a soap shop in Kandahar, Afghanistan; 1331, *ishghar* from Herat glass factory in Fayzullah, Afghanistan, and 1381, *keli* prepared from the chinan desert plant; were prepared by local workers and have an unknown heating history.

Ash sample 1330 was selected for XRD analysis to detect carbonate phases present in the ash (Fig. 11). The ashes are poorly crystallized resulting in heavy background noise on the XRD patterns. The lack of any outstanding major phases makes distinguishing peaks from the background noise difficult. However, certain carbonate phases were sought based based on XRD analysis of ashes done by Stapleton (2003). Trona, nyerereite, $\text{Na}_2\text{Ca}(\text{CO}_3)_2$, magnesite (MgCO_3) and sodium carbonate were detected in the ash samples (Fig. 11).

The plant ash samples were also subjected to TGA to determine the temperatures of volatile loss. Full heating during TGA, to 900°C, volatilized about 50% of the samples. Sample 1331 shows two small peaks (Fig. 12a) below 200°C related to water loss. The total on the analysis of sample 1331 is low (Table 1c) reflecting the presence of some water. The gradual decline in wt% shown on the 1331 TGA curve is probably related to the gradual decomposition of poorly-crystallized carbonate phases in the ash. Sample 4417 has a clearly defined peak in

the TGA curve near 886°C (Fig. 12b) related to carbonate decomposition or melting of a sulfate phase.

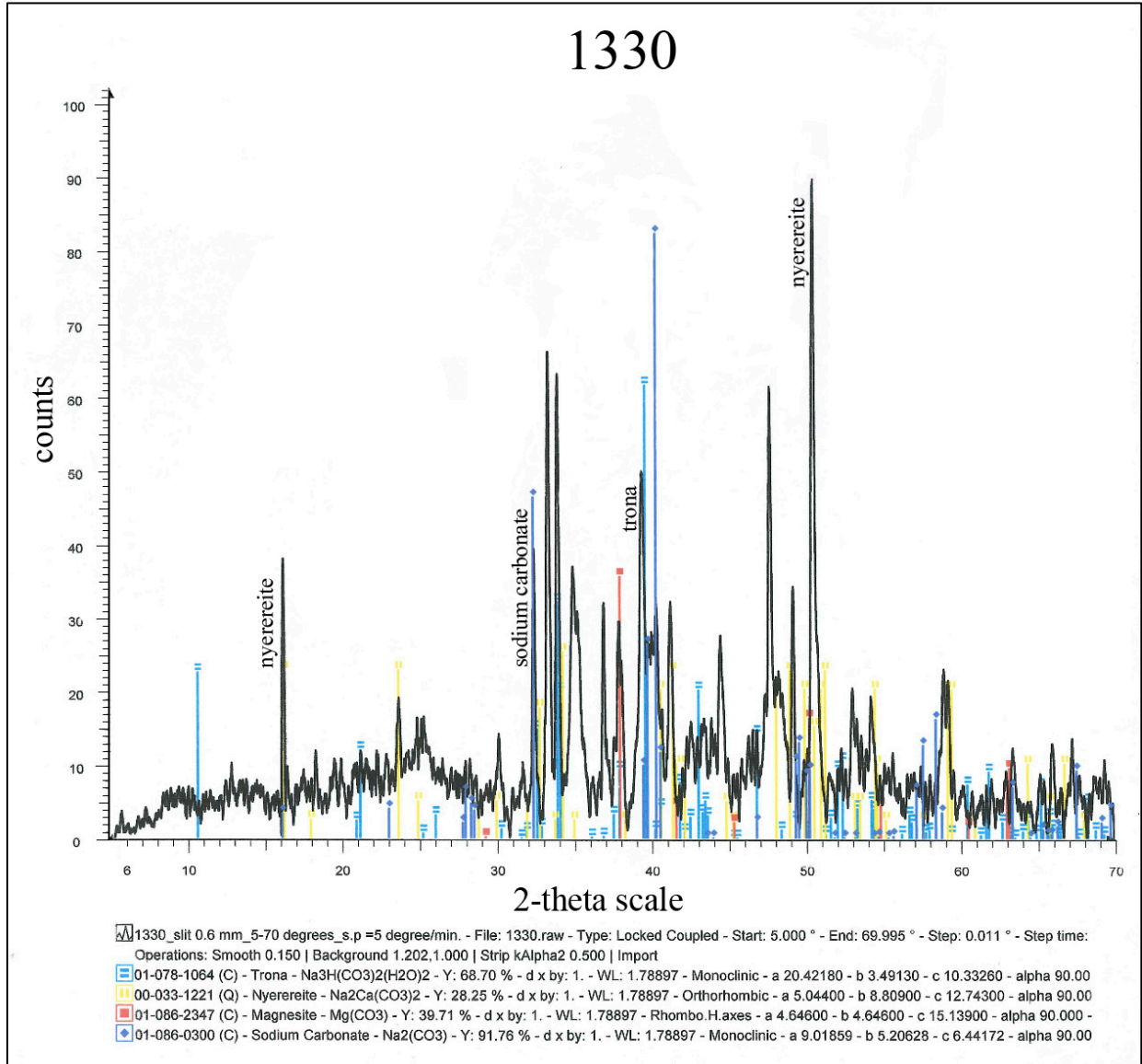


Figure 11. XRD pattern of plant ash 1330.

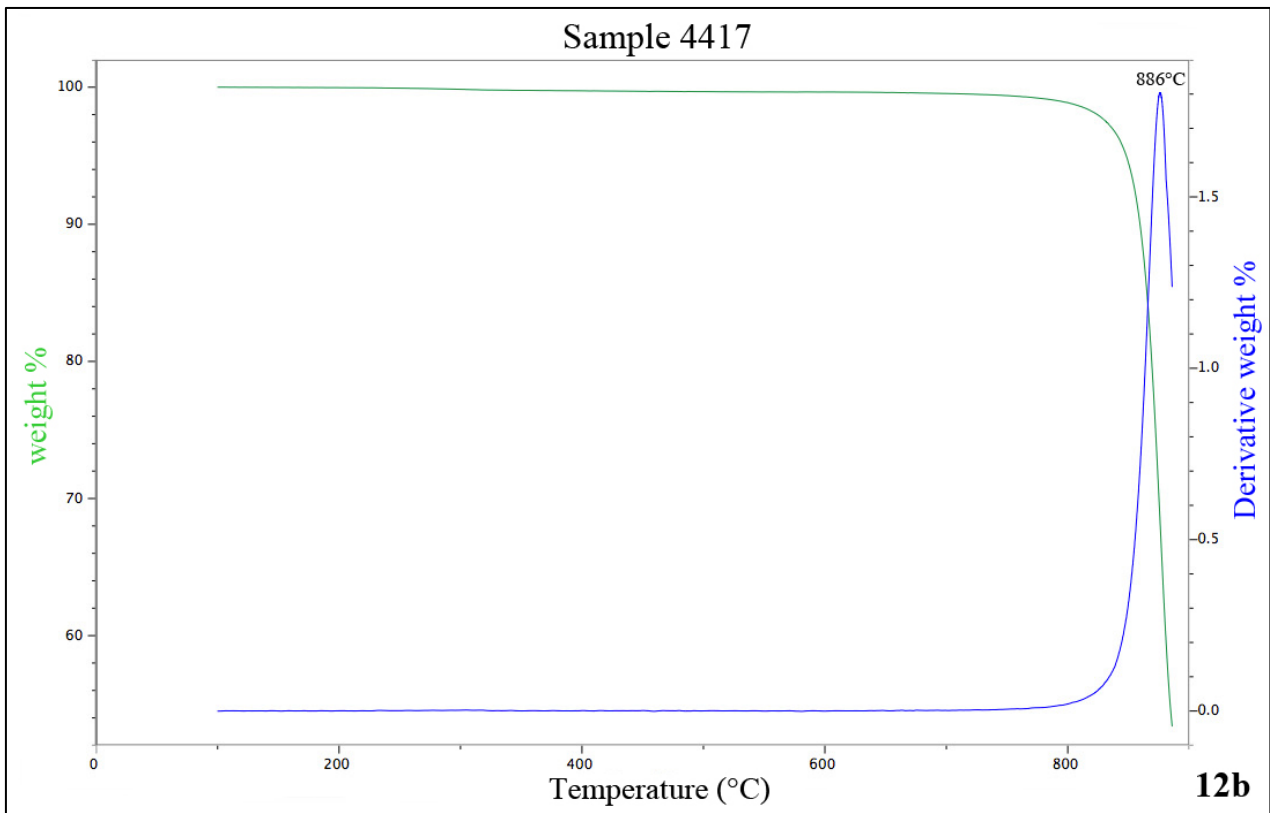
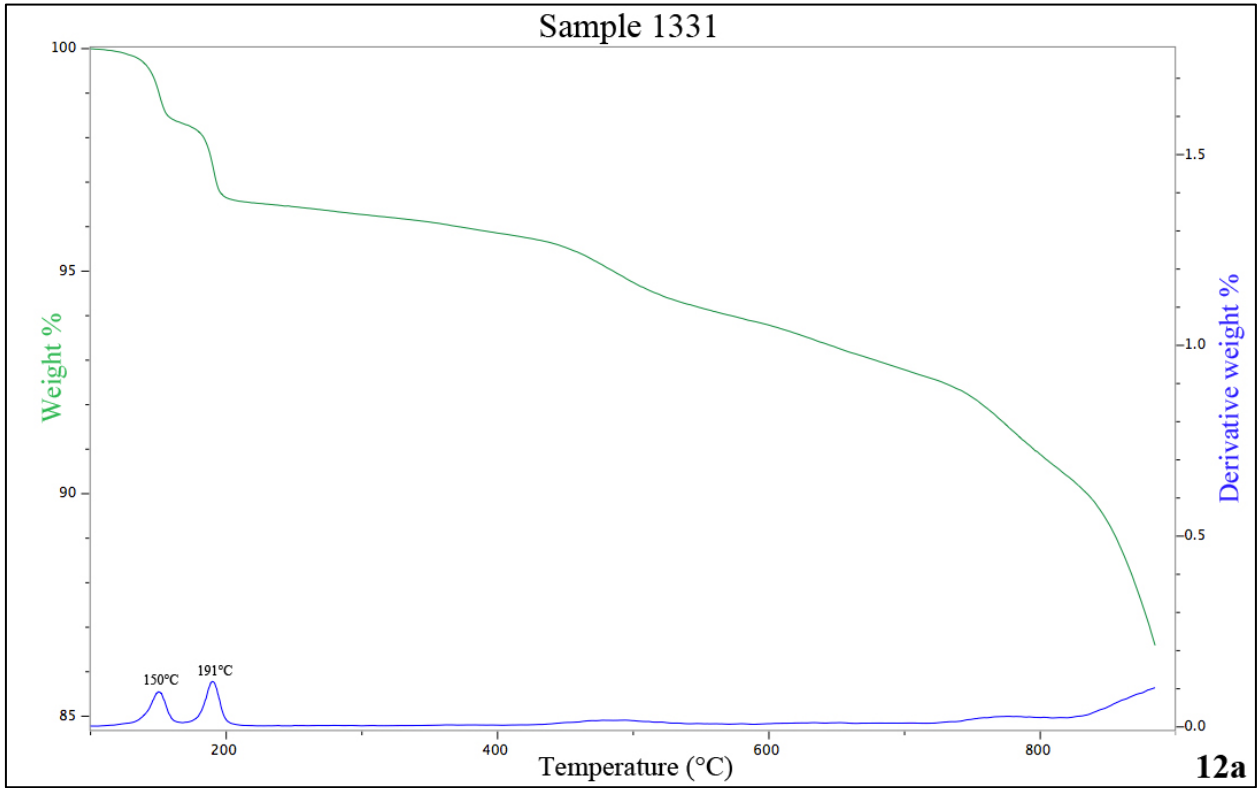


Figure 12. TGA results from ash samples 1331 and 4417

Glass-making Experiments

Prior to mixing any raw materials, phase diagrams were consulted in order to determine the necessary proportions of quartz and alkali that would yield a melt at 1100°C, the target high temperature of the experiments (Fig 13). This temperature was chosen because 1100°C was an achievable temperature for melting glass during ancient times (Henderson 2002; Lilyquist and Brill 1993). The Spruce Pine quartz and chosen alkali were ground into fine powders using a porcelain mortar and pestle with ethanol and dried before being weighed out and mixed together.

Anionic components from the alkali source affect the melting behavior. In the ashes, chloride (Cl), sulfate (S) and carbonate (CO₃) are all present in variable amounts. The Corning mineral alkalis contain abundant Cl, while the Solvay trona contains carbonate and water. Sulfate phases were detected in XRD analyses of mineral alkalis (326, Fig. 4; 656, Fig. 6; 658, Fig. 7) and S is present in many of the ash analyses (Table 1c). Heating results in melting of the sulfate phases (sodium sulfate melts at 884°C) and incorporation of cations (Na⁺) and anions (SO₄⁻²) into the silicate melt. Assuming an oxidizing melt environment, as in the experiments in this study, the sulfate eventually decomposes with the loss ("boiling") of SO₂ gas from the melt producing foam of melt and gas. Depending on the rate of heating, the foaming may be violent and the foam may spill-over the melting crucible (Kim and Hrma, 1992).

A series of experiments (runs 33-38, Table 3) were done with Solvay trona and quartz and illustrates the utility of the phase diagrams in selecting glass-forming compositions. Several batches, with varying SiO₂/Na₂O ratios, were prepared to span the range of melting compositions predicted by the Na₂O – SiO₂ phase diagram (Fig. 13). Upon heating, Trona initially decomposes to Na₂CO₃ and gaseous CO₂ and H₂O. The Na₂CO₃ decomposes at about 850°C to yield Na₂O and CO₂. The trona and quartz were mixed in small amounts and then placed in

ceramic crucibles, heated at 5°C/min up to 700°C, and soaked for 10 hours before shutting off furnace power and cooling to ambient conditions. This stage in the glass-making process is called fritting and is important for driving off gaseous impurities, making the final glass more stable (Henderson 2000a). The resulting frits were ground down to fine powders once again and then wrapped in platinum foil for the final stage of heating. The foil wrapped samples were then placed in a cold furnace and heated at 5°C/min up to 1100°C, soaked for 10 hours, and allowed to cool to room temperature. The furnace has an oxidizing atmosphere, open to the surrounding air. After the final firing, each product was examined under cross-polarized light using a petrographic microscope to determine the extent of melting that occurred and the presence or absence of impurities.

Results of the reconnaissance experiments confirm the results predicted by the phase diagram (Fig. 13). The experiments that plotted in the liquid field melted, however experiments 36-38 contained crystals and some partially melted quartz. Experiment 35 was the only successful run with the WY trona. The successful glass experiments are those that were fully melted and had no or very few impurities.

Successful glass-making experiments are described in Table 4. These experiments, designed to produce 1-2 grams of glass for isotope analysis, were done in platinum crucibles. Run 35 was replicated using larger amounts of trona and quartz. Subsequent references to run 35 refer to this larger batch of glass.

Table 3. Descriptions of glass experiments

Run	Alkali	Quartz (g)	Alkali (g)	frit T(°C), t(hrs)	melt T(°C), t(hrs)	results
16	323	0.6	0.7	na	1100, 10	crystals + glass
29	323	0.158	0.213	700, 10	1000, 10	crystals + glass
30	323	0.1	0.203	700, 10	1000, 10	crystals + glass
11	324	0.65	0.70	na	1000, 10	crystals + glass
14	324	0.65	0.70	1000, 10	1100, 10	crystals + glass
17	324	0.5	0.70	na	1100, 10	crystals + glass
19	324	0.32	0.32	na	900, 10	crystals + glass
10	326	0.65	0.70	na	1000, 10	crystals + glass
15	326	0.65	0.70	1000, 10	1100, 10	glass
9	655	0.65	0.69	na	1000, 20	crystals + glass
23	656	0.7	0.50	900, 10	1100, 10	crystals + glass
24	656	0.7	0.50	1000, 1	1100, 1	crystals + glass
8	658	0.65	0.841	na	1000, 20	crystals + glass
22	658	0.7	0.50	900, 10	1100, 10	crystals + glass
33	WY	4.5	1.22	700, 10	1100, 10	unmelted
34	WY	4	2.43	700, 10	1100, 10	unmelted
35	WY	3.5	3.65	700, 10	1100, 10	glass
36	WY	3.25	4.25	700, 10	1100, 10	crystals + glass
37	WY	3	4.86	700, 10	1100, 10	crystals + glass
38	WY	2.5	6.08	700, 10	1100, 10	crystals + glass
32	650	0.484	0.243	750, 10	1100, 10	crystals + glass
13	1324	0.461	0.398	na	1100, 10	crystals + glass
6	1326	1.27	1.0	na	1100, 10	glass
7	1330	2.36	2.0	na	1100, 10	glass
20	1331	0.54	0.50	900, 10	1100, 10	glass
12	1381	0.71	0.50	na	1100, 10	glass
21	4413	0.372	0.362	900, 10	1100, 10	glass
26	4417	0.7	0.60	na	1100, 10	crystals + glass
31	A 4417	0.595	0.294	na	1100, 10	crystals + glass

Na₂O-SiO₂

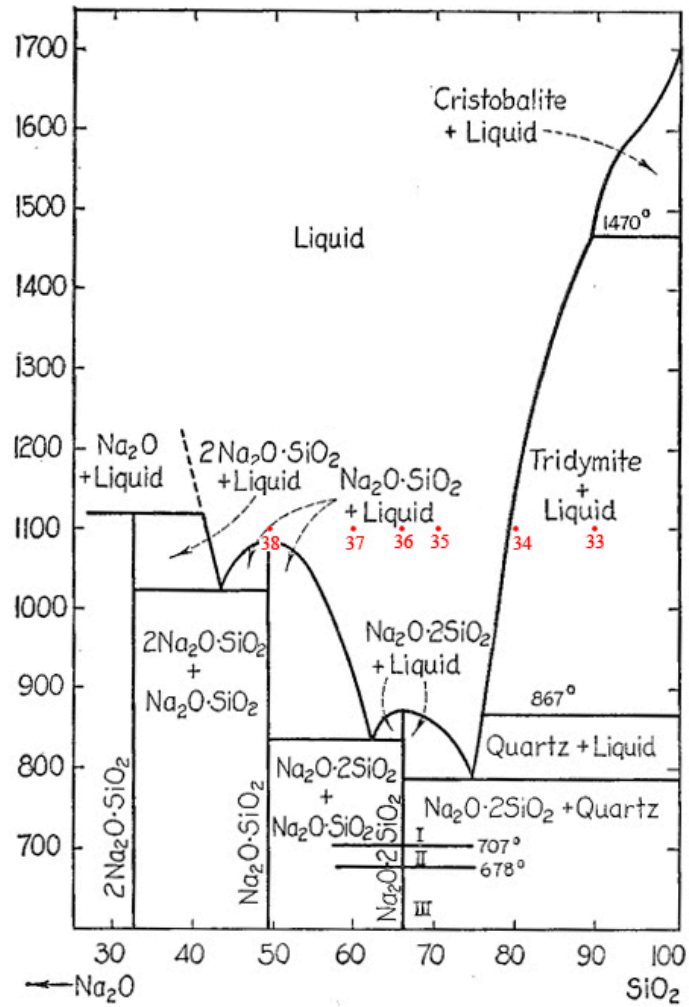


Figure 13. SiO₂ - Na₂O phase diagram with WY trona reconnaissance experiments plotted in red (after Kracek 1930)

Table 4. Table of successful glass experiments

Run #	CMOG alk #	gm alk	gm qtz	gm CaCO ₃	run T (°C)	Comments
6	1326	1	1.27	0	1100	clear glass, few bubbles
7	1330	2	2.36	0	1100	clear glass, few bubbles, few brown unmelted grains
12	1381	0.5	0.71	0	1100	clear glass, few bubbles
13	1324	0.4	0.45	0	1100	lt. brown vesicular glass+ tetragonal crystals (not melted)
15	326	0.7	0.65	0	1100	clear glass
20	1331	0.5	0.54	0	1100	clear, colorless glass
21	4413	0.36	0.72	0	1100	clear, colorless class
35	WY*	.30	.70	0	1100	Clear, colorless glass

Mineral alkali sources contain Na as the major cation (Table 1a and 2). Melting relations for quartz-mineral alkali mixtures are described by a Na₂O – SiO₂ phase diagram (Fig. 13). Ash alkali sources contain Na, K, Mg, and Ca, but Na is the major component (Table 1c). Melting relations of the quartz – ash experiments were modeled in the system CaO – Na₂O – SiO₂ plus 5 wt. percent MgO (fig. 14). This system was derived to model melting in glass-forming systems (Shahid and Glasser 1972) and works well for the experiments involving ash.

Plant ash alkali sources contain variable amounts of chloride, sulfate, and carbonate anions (Table 1c). Carbonates do not present a problem for glass formation, as explained earlier. Chloride does present a problem due to the formation of Cl-rich and Si-rich immiscible melts. Several of the experiments produced immiscible melts with varying degrees of crystallinity. These mixed glasses were not used in this study.

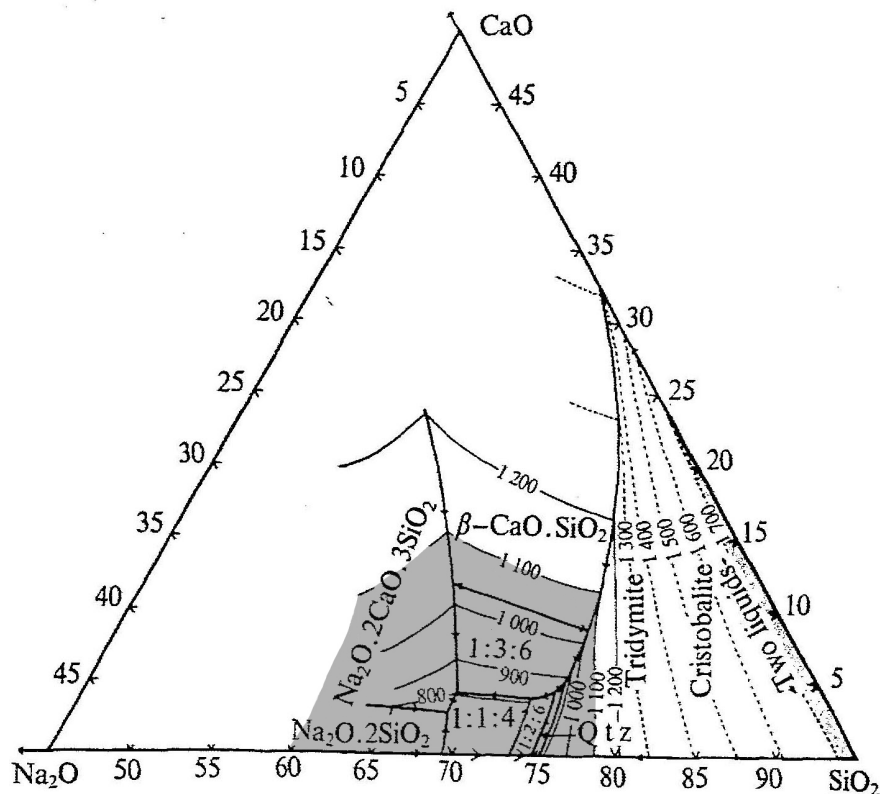


Figure 14. Liquidus phase diagram for a portion of the system $\text{Na}_2\text{O} - \text{CaO} - \text{SiO}_2$ with 5 wt% MgO. The 1100 isotherm is highlighted in red (after Shahid, and Glasser 1972).

Sulfur also forms immiscible, S-rich droplets in a Si-rich melt (Stapleton and Swanson 2002), but the chemistry of sulfur is dependent on the oxidation state of the system. The glass-forming experiments were done in an open-air atmosphere that should, ultimately, produce oxidation of the sulfur and the formation of some gaseous sulfur dioxide. Sulfur is not expected in the glasses formed at 1100°C in these experiments.

Electron Microprobe Analysis

Eight experimental glasses were analyzed using the electron microprobe at the University of Georgia. Small shards of glass were chosen based on their size and shape, and then mounted in epoxy and left to dry for 24 hours. Each mount was sanded with 600-grit for a minimal amount of time, only until the glass shards were just exposed at the surface. Any further sanding would create indentations in the mounts because the glass samples are softer than the surrounding epoxy. Water was not used at all during the sanding or polishing stages, as it is

likely that some of the Na-rich glass samples could be soluble in water. The epoxy mounts were then polished with a diamond hydrocarbon suspension at 15-minute intervals using 3 μ and then 1 μ diamond polishing compound. The mounts were examined after each 15-minute interval until a uniform polish was reached. The polishing process took approximately 1 hour per mount, 30 minutes at 3 microns and 30 minutes at 1 micron. The mounts were then thoroughly cleaned with ethanol to remove any hydrocarbon residue before being carbon coated for EMPA.

A JEOL 8600 microprobe with 4 wavelength dispersive spectrometers was used to analyze the glasses in this study. The accelerating voltage was 15kV, with a beam current of 2 nA and a beam diameter of 15-20 μ m. Tektite glass was used for the calibration of SiO₂ rather than quartz, because it is 65% SiO₂, which is slightly less than the expected concentration in the glasses. An albite standard containing approximately 11% Na₂O served as a standard for Na₂O. Corning glass standards A and B were also analyzed in order to determine the precision and accuracy of the instrument prior to analyzing the glasses. The counting times for each element were 20 seconds. Although a short counting time is not ideal to achieve the most accurate measurements, the counting time had to be kept short to minimize beam damage on the Na-rich glass samples due to Na volatilization. Beam damage can result in inaccurate measurements, so 20 seconds was chosen in an effort to find a middle ground between the two issues. The results from the EMPA analyses are summarized in Table 5.

Table 5. Representative analyses of EMPA results for successful glass experiments.

Run	6	7	35	12	13	15	20	21
Alkali source	1326 ash	1330 ash	WY trona	1381 ash	1324 ash	326 natron	1331 ash	4413 ash
SiO ₂	70.94	67.90	69.59	71.84	72.12	67.62	73.77	70.70
TiO ₂	0.05	0.08	0.04	0.05	0.26	bdl	0.03	bdl
FeO	bdl	0.10	0.43	0.19	1.58	0.07	0.35	0.21
Al ₂ O ₃	0.20	0.39	0.87	0.74	2.49	0.47	1.56	1.01
MgO	5.22	5.90	4.37	3.75	3.29	3.75	0.84	2.30
CaO	3.83	6.37	5.97	10.09	9.25	6.38	1.21	3.79
MnO	bdl	0.43	bdl	0.24	bdl	0.01	bdl	bdl
K ₂ O	2.57	7.22	1.71	1.36	1.88	8.98	0.40	4.69
Na ₂ O	16.82	9.78	16.26	11.34	9.05	10.77	17.32	14.04
SO ₃	0.13	0.16	0.10	0.21	0.08	0.06	0.11	0.08
Cl	0.06	0.35	0.79	0.08	0.17	0.04	0.03	0.03
TOTAL	99.74	98.69	99.87	99.89	100.11	98.09	95.00	96.54

Bdl = below detection level

Oxygen Isotope Analysis

Oxygen isotope analysis was performed on the raw plant materials, ashes and mineral alkalis, fritted alkalis, and the final glasses. All the samples, except for the glasses, were pulverized to a very fine grain size prior to analysis. The plant isotopes were run using a continuous flow High Temperature Conversion Elemental Analyzer (TCEA) system at the University of Arkansas Stable Isotope Laboratory. This system combusts samples at very high temperatures in a reduced environment, converting the oxygen to CO. Samples are placed in silver capsule and pyrolyzed at 1400°C. The CO is separated on a 1 M 5A mol sieve GC column and run through a Finnigan DELTAplus XP IRMS (Isotope Ratio Mass Spectrometry) system. A more detailed description of the pyrolysis method is given in Gehre and Strauch (2003).

The alkalis (ash and minerals), Spruce Pine quartz, and glasses were analyzed using a laser fluorination system at the University of Georgia Stable Isotope Laboratory by a method modified from Valley et al. (1995). At least two 2-3 mg aliquots of each sample was measured and packed into sample cups. In the case of the glass, glass shards were chosen based on best fit for the cup. The cups were loaded into the laser chamber and then individually reacted with the fluorination agent, BrF_5 . The BrF_5 is released into the chamber while the sample is heated with a variable power CO_2 laser (Synrad, 10510-10650 nm wavelength, 75W max power). The resulting reaction releases the O_2 , which is then converted to CO_2 by passage over heated graphite. The CO_2 is then transfer to a Finnegan MAT 252 mass spectrometer for analysis. Sample analyses were accompanied by standard mineral analyses NBS-28 (quartz sand) and UWG (garnet) to assure accuracy and precision of the unit. NBS-28 was used as a standard for the Spruce Pine quartz and UWG for all other samples. The results and error analysis from the isotope analyses are presented and discussed in the following section.

RESULTS

Glass-making Experiments

Thirty-eight experiments were made in attempts to make glass with the available materials. All experiments used the Spruce Pine quartz as the glass-forming component and either a mineral-alkali (natron or trona) or a plant ash alkali as the network modifier. The experimental glasses made with mineral alkalis do not contain any added lime, which was sometimes used as a stabilizer in ancient glasses (Henderson 2000a). As a result the Na-rich glasses made with mineral alkalis are soluble in water. The glasses were prepared approximately 60% network former (quartz) to 30% network modifier (alkali).

Table 3 shows all the glass experiments that have been done at UGA to date. Some of the mineral alkalis consist mainly of halite. Chloride phases do not decompose upon heating, but melt to form a Cl-rich immiscible melt (Tanimoto and Rehren 2008). These alkalis are unsuitable for glass making (Henderson 2013). The alkali sources that were successful in mixing with the quartz to make glass had at least some amount of sodium carbonate. Sodium carbonate decomposes upon heating allowing for a larger portion of the sodium to react with the quartz (Henderson 2013).

The proportions of the alkali and silica components in the glass experiments were plotted on a $\text{SiO}_2 - \text{Na}_2\text{O} - \text{CaO}$ phase diagram that also accounts for 5% MgO (Fig. 14). Batch compositions that plotted in the liquid field between 1000-1100 °C generally resulted in successful glass-making experiments. A full procedure for the glass experiments is described in the methods section. The successful glass-making experiments are summarized in Table 4. The

glasses were mostly clear and colorless, with the exception of experiment 13, which was a light brown color with small inclusions.

Glass Compositions

Glass standards, Corning A and Corning B from CMOG, were used to determine the accuracy and reproducibility of EMPA of glass. The Corning Glass standards analyzed in this study are compared to equivalent analyses done by Stapleton (2003), as well as to the recommended compositions by Brill (1999) (Table 6). Our analyses show lower values for Na₂O in both standards than the recommended values and those done by Stapleton (2003). Precision is given by the relative standard deviation (RSD) in Table 6.

Table 6. Comparison of Corning Museum Glass Standards

Corning A						Corning B					
	Brill (1999)*	Stapleton (2003)	This study	SD	RSD[†]		Brill (1999)*	Stapleton (2003)	This study	SD*	RSD[†]
SiO₂	66.65	67.66	70.57	2.04	1.96	SiO₂	61.55	62.23	61.62	0.37	0.40
TiO₂	0.79	0.84	0.87	0.04	3.35	TiO₂	0.089	0.21	0.14	0.06	32.73
Al₂O₃	1	0.92	0.83	0.08	6.34	Al₂O₃	4.36	4.45	4.07	0.20	3.13
FeO	0.98	1.05	1.14	0.08	4.89	FeO	0.31	0.38	0.31	0.04	8.98
MnO	1	0.91	0.90	0.05	3.85	MnO	0.25	0.4	0.37	0.08	16.04
MgO	2.66	2.75	2.60	0.08	1.93	MgO	1.03	1.08	1.09	0.03	2.03
CaO	5.03	5.1	5.19	0.08	1.07	CaO	8.56	8.95	9.03	0.25	1.88
Na₂O	14.3	14.75	12.48	1.20	6.12	Na₂O	17	17.6	15.23	1.23	5.20
K₂O	2.87	2.66	3.13	0.23	5.11	K₂O	1	1.01	1.20	0.11	6.59
P₂O₅	0.13	bd	ns			P₂O₅	0.82	0.91	ns		
SO₃	0.16	bd	0.18	0.01	5.60	SO₃	0.54	0.44	0.44	0.06	8.24
Cl	0.1	0.1	0.12	0.01	5.82	Cl	0.2	0.18	0.19	0.01	3.44
Sb₂O₅	1.75	1.79	ns			Sb₂O₅	0.46	0.54	ns		
CuO	1.17	1.2	ns			CuO	2.66	2.93	ns		
PbO	0.12	bd	ns			PbO	0.61	bd	ns		
CoO	0.17	bd	ns			CoO	0.046	bd	ns		
total	98.88	99.73	98.02			total	99.485	101.31	93.69		

* Recommended compositions

SD - Standard deviation between all three studies

RSD – Relative standard deviation from recommend values (Brill 1999). RSD = 100* SD/mean

bd = below detection level

ns = not sought during analysis

Overall the precision of our analyses are well within 10% for all the major elements (>1 wt%). The minor elements (<1 wt%) have much higher RSD values, which is attributed to low count rates produced by the low beam current during analysis. Discrepancies between the values in this study, and those done by Stapleton in 2003, are attributed to software updates to the EMPA, and the use of different standards for Na₂O.

Glasses made in this study were analyzed by EMPA (Table 5). Stapleton (2003) also reported EMPA of glasses from experiments 6 and 7 and her results are compared to results in this study in Table 7.

Table 7. EMPA Results of Glasses 6 and 7 from this study and Stapleton (2003)

	Glass 6			Glass 7		
	Stapleton (2003)	This Study	Std dev	Stapleton (2003)	This study	Std dev
SiO ₂	68.07	70.94	2.0	65.14	67.90	1.95
TiO ₂	bd	0.05		bd	0.08	
FeO	bd	bd		bd	0.10	
Al ₂ O ₃	0.25	0.20	0.04	0.47	0.39	0.06
MgO	5.66	5.22	0.31	6.76	5.90	0.61
CaO	3.73	3.83	0.07	6.79	6.37	0.30
MnO	bd	bd		bd	0.43	
K ₂ O	2.39	2.57	0.13	6.57	7.22	0.46
Na ₂ O	18.76	16.82	1.37	10.75	9.78	0.69
SO ₃	0.35	0.13	0.16	0.32	0.16	0.11
Cl	0.67	0.06	0.43	0.46	0.35	0.08
TOTAL	100.18	99.74		98.29	98.69	

Expected compositions for the glasses were calculated based on proportions of quartz and alkali added to the batch. The chemical analyses of the alkali sources were taken from Brill (1999). The expected compositions were then compared to the compositions measured during EMPA analysis (Table 8). This comparison allowed for the detection of unexpected changes to the composition of the raw materials during the glass-making process. Generally, there is good correspondence between the expected and actual glass analyses. Some loss of Na is expected

during preparation of the glass and during the EMPA yet Na analyses show no systematic variation (Table 8).

Table 8. Comparison of expected vs. measured glass compositions

Run	Wt%	SiO ₂	TiO ₂	Al ₂ O ₃	Fe ₂ O ₃	MnO	MgO	CaO	Na ₂ O	K ₂ O	Total
6	Expected	73.67	0	0.17	0.12	0	4.80	1.85	16.67	2.72	100
	Measured	70.94	0.05	0.21	bdl	bdl	5.22	3.83	16.82	2.57	99.64
7	Expected	65.02	0	0.31	0.18	0	7.33	5.95	11.74	9.48	100.01
	Measured	67.9	0.08	0.39	0.10	0.43	5.90	6.37	9.78	7.22	98.17
12	Expected	72.44	0	0.68	0	0	4.20	7.95	8.99	5.73	99.99
	Measured	71.84	0.05	0.74	0.19	0.26	3.75	10.09	11.34	1.36	99.62
13	Expected	75.37	0.32	1.96	1.41	0	3.20	5.52	10.21	1.99	99.98
	Measured	72.12	0.26	2.49	1.58	bdl	3.29	9.25	9.05	1.88	99.92
15*	Expected	63.57	0	0	0	0	0	0	36.43	0	100
	Measured	67.62	bdl	bdl	bdl	bdl	3.75	6.38	10.77	8.98	97.5
20	Expected	76.11	0	0.47	0.16	0	3.59	3.00	14.57	1.88	99.78
	Measured	73.77	0.03	1.56	0.35	bdl	0.84	1.21	17.32	0.40	95.48
21	Expected	64.92	0	0.17	0	0	3.84	5.06	12.39	13.61	99.99
	Measured	70.70	bdl	1.01	0.21	bdl	2.30	3.79	14.04	4.69	96.74
35	Expected	68.60	0	0	0	0	0	0	31.4	0	100
	Measured	69.59	0.04	0.87	0.43	bdl	4.37	5.97	16.26	1.71	99.24

*Run 15 is made with mineral alkali sample 326. 326 is assumed to be NaCl (53% Na₂O)

There are two notable exceptions to the pattern of uniformity. Run 15 used the mineral alkali 326. The calculated glass composition assumed that all of the Na in sample 326 (Table 2) entered the silicate glass. However, sample 326 is mostly halite and the formation of a Cl-rich melt was to be expected. At the end of the glass-making experiment, the sides of the crucible (inside and out) were coated with a thin film of glass. The puddle of glass at the bottom of the

crucible was sampled for EMPA and determination of oxygen isotopes. The Cl-rich character of the alkali source and the presence of two glasses (side-coating and puddle) at the end of the experiment suggest the presence of two different melts. Subsequent analyses were on just one of these melts.

Run 35 (Tables 1 and 8) used the Wyoming trona as the alkali source. The expected glass composition (Table 8) was calculated assuming the trona was pure. The presence of Mg and Ca in the glass analysis (Table 5 and 8) shows these components must be present in the trona sample. The high Na content of the expected glass versus the lowered measured Na is probably related to impurities in the Wyoming trona.

Figure 15 shows the measured MgO against K₂O content of the experimental glasses. The fields where natron and plant ash glasses should plot according to Brill and Lilyquist (1996) are also plotted. Only one glass, run 6, plots within its expected field. The two mineral alkali glasses (15 and 35) plot very far from their expected fields. Glass experiment 35 was made with the WY Trona. This trona is reported to be 90-93% pure with up to 10% H₂O insolubles. The elevated magnesium in the glass is likely related to the impurities in the trona. Glass 15 was made with the modern Wadi Natrun sample and plots very far from the expected field. This may be the result of a bad analysis. The plant ash glasses are slightly less variable, but still do not plot in the expected field. Halophytic plants have variable amounts of K₂O and MgO depending on their geographic location so it is expected that these glasses would have variable K₂O and MgO contents.

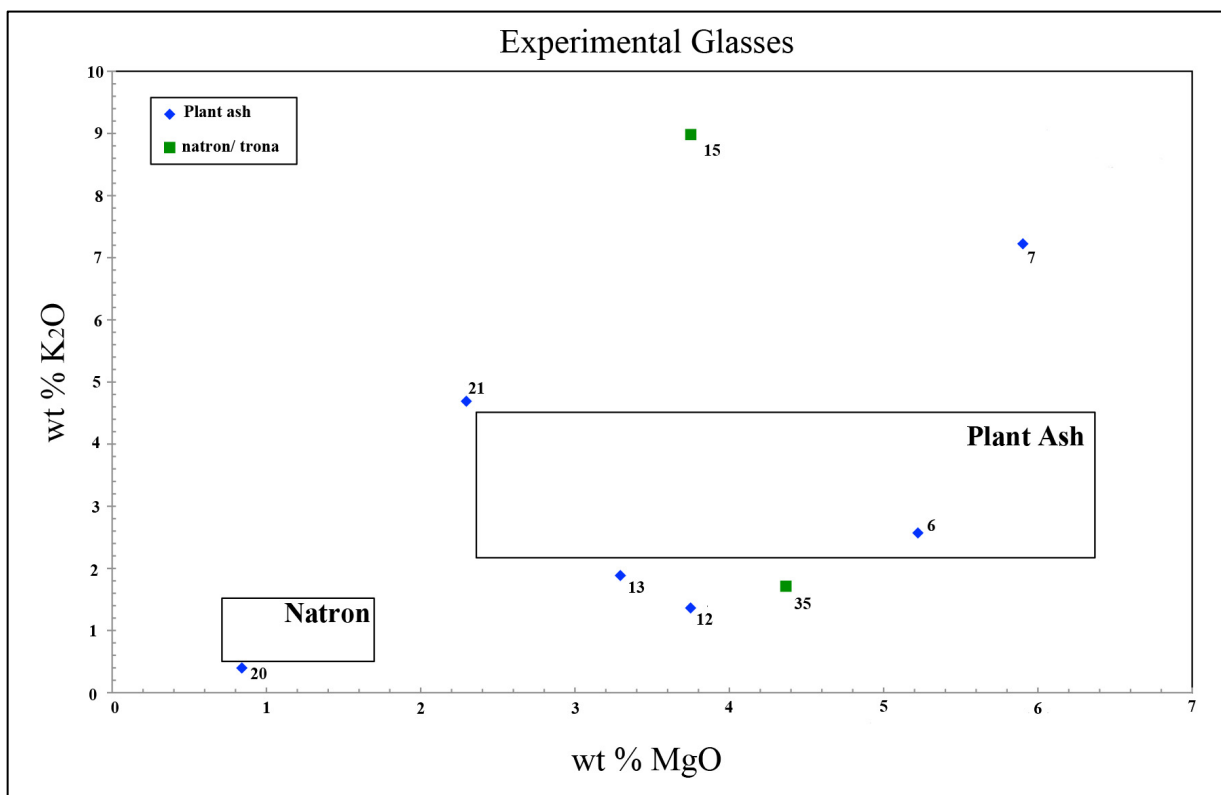


Figure 15. Plot of MgO against K₂O for the experimental glasses based on EMPA. Fields are for plant ash and natron glasses according to Lilyquist and Brill (1996).

Oxygen Isotope Analyses: Plants and Ashes

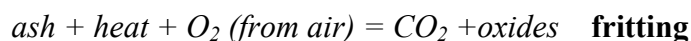
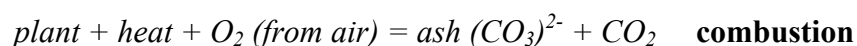
The plant samples have uniformly high $\delta^{18}\text{O}$ values, ranging from 22 to 39 (Table 9). Leaves (sample 651, Table 9) and stems (sample 650, Table 9) from the same plant have the same oxygen composition. Plant 1326 (Iraq) and 1380 (Afghanistan) have the highest oxygen $\delta^{18}\text{O}$ (Table 10). Other plants have similar oxygen isotope compositions in the 20-30‰ (Table 10).

Table 9. Oxygen isotope ratios for halophytic plants

CMOG catalog #	$\delta^{18}\text{O}$ (VSMOW)
650	22.08
651	21.91
1324	28.58
1326	39.23
1380	35.94
4402	25.48
4413	27.13
4416	22.89

The plant materials and corresponding ashes were analyzed for ^{18}O -content at the University of Arkansas and the University of Georgia Stable Isotope Laboratories, respectively. The results of these analyses are summarized in Tables 9 and 10. Two samples (1326 and 1380, Table 11) are represented by analyses of the plant and the ash.

As can be seen in the data, the ^{18}O -content of the ashes is drastically lower than the plants, suggesting a change in the isotopic composition during the combustion process. The ashes were heated to 900°C to simulate the first stage of heating (“fritting”) during glass-making and analyzed again (Table 10 and 11). The fritted plant ashes produced between 10-40 μmol of CO_2 . The resulting ^{18}O -contents were lower than the unheated ash samples. The systematic lowering of the $\delta^{18}\text{O}$ ratio is related to the following reactions:



Every step in heating of the plant ash alkalis breaks down carbonates and drives off CO_2 , therefore causing the $\delta^{18}\text{O}$ ratio to systematically decrease. The compounding effect of heating is shown in the isotope ratios of the plants, ashes, fritted ash, and glasses in Table 11.

Table 10. Oxygen isotope ratios of raw materials, fritted alkalis and experimental glasses

Material	Sample wt. (mg)	n	$\delta^{18}\text{O}$ (VSMOW)	stdev*
ASHES				
1326	1.8		17.7	
1330	2.7		12.6	
1331	nr		11.7	
1381	4.0		16.4	
NATRON/TRONA				
326	2.9		9.7	
WY Trona	2.1		15.4	
QUARTZ				
SP QTZ	2.48	6	11.7	0.3
FRITTED ALKALIS[†]				
1326-900	nr	2	11.4	0.3
1330-900	nr	3	8.5	0.9
1331-900	nr	3	8.7	0.3
1381-900	nr	3	7.9	1.3
326-900	3.27	2	7.8	0.4
WY TRONA-900	2.2	2	9.3	0.06
4413 ^{††}	1.5		5.6	
GLASSES				
RUN 12 (<i>1381</i>)	3.0	2	9.7	0.2
RUN 13 (<i>1324</i>)	2.9	2	9.7	0.0
RUN 15 (<i>326</i>)	2.5	2	9.5	0.1
RUN 20 (<i>1331</i>)	2.8	3	9.8	0.2
RUN 21 (<i>4413</i>)	2.4	2	9.8	0.0
RUN 6 (<i>1326</i>)	2.5	2	10.0	0.5
RUN 7 (<i>1330</i>)	2.5	2	10.2	0.2
RUN 38 (<i>WY trona</i>)	2.1	2	10.0	0.1

*Data in **bold** are averages of n repeat analyses **stdev = standard deviation from averaged data.

[†] Alkalis were fritted at UGA, samples were heated to 900°C and soaked for 10 hours. ^{††} Sample 4413 was pre-fritted at CMOG. The alkali used in the glass experiments is given in parentheses next to the run number. nr = not recorded

Table 11. Comparison of oxygen isotope ratios for plants, ashes, fritted ashes, and plant ash glasses

CMOG #	Plant	ash	Fritted	glass
1324	28.58	na	na	9.69
1326	39.23	17.71	11.4	10.04
1330	na	12.62	5.51	10.19
1331	na	11.70	8.7	9.77
1380	35.94	16.37	6.89	9.67
4413	27.13	na	5.57	9.80

na = not analyzed due to insufficient amount of material

Oxygen Isotope Analyses: Mineral Alkalis

Most of the mineral alkalis from the CMOG collection were not successful in the glass-making experiments. Only one successful glass experiment (15) has been made from mineral alkali sample 326 (Table 1a). This alkali source has a very high concentration of Na₂O, although most of the Na is in the minimally reactive form of halite. The Wyoming trona contains little to no NaCl and was therefore very successful in the glass-making experiments

Oxygen isotope analysis by laser fluorination was conducted only on the samples 326 and WY trona, as these are the only samples that have produced a clear glass; the results are summarized in Table 12. Analyses produced low amounts of CO₂ (3.0 μmol) for sample 326, reflecting the high halite content of the sample. The Wyoming trona produced more CO₂ (9.4 μmol), reflecting the higher carbonate content of this alkali source. The results show that the oxygen isotope ratios decrease with increasing temperature.

Table 12. Oxygen isotope results for the mineral samples, heated mineral, and final glass.

Sample #	Mineral alkali	Mineral alkali at 900°C	Glass
326	9.7	7.8	9.5
WY trona	15.4	9.3	10.0

DISCUSSION

Composition of Raw Materials

Quartz

The Spruce Pine quartz that was used in all of the glass-making experiments is considered to be pure quartz. Glassmakers during ancient times would traditionally use beach sands as the glass-former component because it also contained lime in the form of shells that served as a stabilizer in the glass. Pure quartz was used because it is uniform in composition and has a consistent $\delta^{18}\text{O}$ ratio. Six isotope analyses were run on the Spruce Pine quartz and all of them produced $\delta^{18}\text{O}$ ratios of 11.7‰.

Mineral Alkalis

Mineral alkalis 326, 656, and 658 contain abundant halite (Figures 4, 6 and 7). In the presence of abundant Cl, melting of Si-rich compositions yields mixtures of Cl-rich and Si-rich melts are known to be immiscible (Henderson 2013). Alkalis (Na, K) partition between the two melts, forming one melt rich in Cl and one melt rich in Si. Several glass-making experiments in this study produced immiscible melts with a clearer glass below an opaque, bubbly crust (Henderson 2013). Apparently, a fractionation is occurring in the melt, where the immiscible fluids are separating during heating, creating a Cl-rich crust over a silica-rich glass. (Stapleton 2003, Henderson 2013).

Samples 655, 656 and 658, from the tomb of King Tutankhamen, are assumed to have been collected from Wadi el Natrun during late 13th century BC (Brill 1999). The samples are high in Na and Cl (Table 1a). Salts from Wadi el Natrun were also used for embalming

mummies (Henderson 2002, 2013). Embalming salts are rich in halite, explaining why most of the tomb samples have not been successful in the glass-making experiments (Shortland et al. 2011, Henderson 2013).

Shortland (2004) and Shortland et al. (2011) provide evidence for seasonal and annual variation in evaporite compositions at Wadi el Natrun. The halite-rich tomb alkali sources were collected at a time when the evaporate product was rich in halite (the desired component for embalming). It is likely that the compositions of the evaporite minerals that were mined for glass-making during ancient times are very different from those that are present at the lakes today (Shortland 2004). This may explain why there has been have had limited success with making glass from the modern Wadi el Natrun alkali samples 323 and 324 from the CMOG collection.

The Wyoming trona does not contain halite and therefore all of the sodium was available to move into and stabilize the silica network. This proxy was successful in that it produced a clear glass with very few crystals or bubbles.

The isotopic values for the mineral alkalis were much lower than expected based on previous works by Brill (1970) and Silvestri et al. (2010). Both studies report oxygen isotope ratios for Wadi Natrun evaporates to be about 40 ‰ $\delta^{18}\text{O}$. Our study found the modern Wadi Natrun sample (326) and the Wyoming trona (WY trona) to be 9.7‰ and 15.4‰, respectively. Part of the explanation may be a difference in analytical technique. This study produced fusion of the mineral alkali samples using a laser beam, while Brill (1970) and Silvestri et al. (2010) used Ni-rod reaction vessels for the extraction of oxygen (Clayton and Mayeda 1963, Silvestri et al 2010). Their samples were placed in the Ni-vessel for between 3-48 hours at temperatures between 500-600°C depending on the material (Clayton and Mayeda 1963, Silvestri et al 2010).

The behavior of mineral alkalis under the laser during laser fluorination analysis was unexpected. Both samples at first seemed to not react to the laser, but then the behavior would quickly change and the sample boiled over the sample holder, leaving excessive residue. The glass and plant ash samples reacted as expected and were completely vaporized by the laser. The behavior of the mineral alkalis in the laser chamber may explain the low yields for 326, which may have resulted in inaccurately low $\delta^{18}\text{O}$ values for this sample. The value for the Wyoming trona is higher, but not as high as the values listed by Brill (1999) or Silvestri (et al. 2010).

Plants and Plant Ash Alkalis

Samples 1380 and 1381 are the only pair of plant and corresponding plant ash that was analyzed by Brill (1999) (Tables 1b and 1c). The chemical data show that the Na_2O decreases by about 10 wt% while the K_2O increases by the same amount in the ash relative to the plant, perhaps related to sodium loss during ashing. Both CaO and MgO show a substantial increase, while Cl and SO_3 decrease by 12 wt%, and 6 wt % respectively.

The plant ash alkalis have been largely more successful for glass making. Glass makers in the film *The Glass Makers of Herat* (1979) selected the sweetest ash to use in glass making, perhaps because these would have contained lower concentrations of halite, which causes fractionation of sodium and immiscible liquids and therefore not good for making glass. (Henderson 2013). Six different plant ashes (1324, 1326, 1330, 1331, 1380, and 4413) have produced clear glasses (Tables 3 and 4). XRD analyses of the ashes identified various sodium carbonate phases, all seemingly in low degrees of crystallinity (Fig. 11). The plant ashes tend to have rather weak diffraction patterns; however, they do show that there is sodium in the form of carbonates rather than halite, making the ashes more suitable for glass-making. The chemical

analyses of the ashes done by Brill (1999) show that all the ashes that have been successful in making glass have less and 10 wt % Cl.

Several workers, Rehren (2000), Barkoudah and Henderson (2006), Tite et al. (2006), and Tanimoto (2007) have focused on the role of the composition of plant ashes in ancient glass and how composition changes from plants and ashes. Barkoudah and Henderson (2006) found that compositional variation of sodium, magnesium, calcium and potassium across plant species to be about 10-30% and relatively consistent; however, the ashed plant samples were found to be much more variable. The magnesium and calcium oxides have a positive correlation in ashes, but the correlation is not found in ancient glasses (Barkoudah and Henderson 2006). This suggests that the calcium: magnesium ratios are altered during the glass-making process (Henderson 2013). Barkoudah and Henderson (2006) note sodium oxalate ($C_2Na_2O_4$) is always present in the dried plants, which at high temperatures (600-650°C) will break down to Na_2O and CO_2 . This should result in simple sodium-rich compounds such as nyerereite ($Na_2Ca(CO_3)_2$) that would be suitable for glass-making; however, such compounds are absent (Henderson 2013). Instead, the alkalis are present in the form of NaCl and KCl. This is attributed to the ionic exchanges in carbonate phases that occur during heating (Henderson 2013).

Composition of the Glasses

Calculations were done in order to estimate expected chemical compositions of the glasses based on the analyses of alkalis done by Brill (1999) and assuming the Spruce Pine quartz is pure SiO_2 . Results are given in Table 7. The measured oxide values differ from the expected (calculated) values most notably in SiO_2 , CaO, Na_2O , and K_2O . These discrepancies

may be due to: analytical error in Brill's (1999) alkali analyses, errors in EMPA analyses, and fractionation of alkalis due to the presence of chlorine.

The accuracy of Brill's chemical analyses for the raw materials is not known. Some of the analyses do not total to 100%, and some are as low as 56%, presumably due to water and other unanalyzed components. Brill suggests that the low totals result from the presence of anions that were not sought during analyses (Brill 1999). If this is the case then the calculated glass compositions should not be affected since these anions are not present in the final glass mixture. Still it is not clear how to deal with these low totals in calculations of expected glass compositions.

Another source of potential error is the probe standard used for Na₂O. The standard, albite, has a lower Na₂O composition (11%) than many of the experimental glasses, which range between 9 and 17 wt % Na₂O. Since the standard has less Na₂O, the standard need to be projected past its known composition to determine the Na content of the high-Na glasses. EMPA of glass standards (Corning A and Corning B) are available and approximate the accepted values given by Brill (1999) and the analyses done by Stapleton (2003) on the same machine (Table 6). Discrepancies between the values in this study and those done by Stapleton in 2003 are attributed to software updates to the EMPA.

The role of chlorine in the glass melt is another source of possible error. If chlorine is present in the batch, two immiscible melts form (Henderson 2013). Fractionation of Na between the two melts affects the Na₂O composition of the Si-rich melt to an unknown extent. Some of the glass experiments have resulted in the formation of two different melts, one that is high in silica, and one that is high in chlorine. The glasses analyzed by EMPA are only of the former and therefore, may have an even lower Na₂O value than expected. Rehren and Tanimoto (2008)

have shown that potassium reacts in the same way, fractionating between the two melts leading to reduced levels of potassium in the Si-rich glasses; this may explain discrepancies in our K₂O values as well. Brill (1970) suggests that only 75% of analytical concentrations of raw materials are reflected in the final glass, which is at least partially due to ionic exchanges with chlorine.

Results of this study show the MgO-K₂O contents of the glasses are clearly dependent on the type of plant used to flux the silica. The ashes tend to be higher in wt % MgO and K₂O than the glasses (Table 1c and 5). The plant ash glasses may not plotting in the designated field because there was simply not enough ash added to the system. The success of the K₂O-MgO classification is attributable to some uniformity on the selection of plant type used in the glass preparation.

Oxygen Isotopes

Investigations by Brill (1970), Henderson et al. (2005), Leslie et al. (2006) attempted to use oxygen isotopes for the characterization of ancient glasses and found that the majority of the isotopic signature (~70%) is contributed by the silica component. Since the alkali accounts for approximately 30% of the isotopic signature in the glass, then oxygen isotopes should be a useful way to discriminate between raw materials in glasses (Leslie et al. 2006).

The plants have a $\delta^{18}\text{O}$ ranging between 22‰ and 39‰ (Table 10) and vary geographically. The corresponding ashes of the available plants (Table 11a) have $\delta^{18}\text{O}$ values that are on average 55% lower than the ratios of the plants prior to heating. This drastic decrease is likely due to the breaking down of sodium oxalate (C₂Na₂O₄) into Na₂O and CO₂ (Barkoudah and Henderson 2006). The combustion and calcination of the plant material happens in an open system, so the CO₂ is lost to the surrounding environment.

When the samples are heated for the second time (in the fritting stage) the $\delta^{18}\text{O}$ ratios drop once again (Table 11a), this time by an average of 44%. Fritting temperatures reached 900°C. Thermogravimetric analysis (TGA) of the ashes (Fig. 9) show that around 850°C the samples begin to volatilize at a very fast rate. At these high temperatures, carbonates are no longer stable and begin to break down, removing a large portion of the oxygen as CO_2 . When the ashes are mixed with the quartz to make glass their $\delta^{18}\text{O}$ ratios are only approximately 25% of the original.

Theoretical $\delta^{18}\text{O}$ values for the plant ashes were calculated using the following mass balance equation:

$$\delta^{18}\text{O}_{\text{glass}} = f_{\text{quartz}} (\delta^{18}\text{O}_{\text{quartz}}) + f_{\text{plant ash}} (\delta^{18}\text{O}_{\text{plant ash}})$$

Where f = the molar fraction of oxygen in the raw materials. Chemical compositions of the plant ashes given by Brill (1999) (Table 1c) were used in these calculations. CO_2 was not included in the molar fraction because it is assumed to be volatilized by the fritting stage. The theoretical and measured plant ash glass oxygen compositions are summarized in Table 13. The measured values are within range of error to the theoretical values (Table 13). The glass from run 6, which was made with ash 1326 is the farthest from the expected value. The fritted $\delta^{18}\text{O}$ value for 1326 was considerably higher than the other fritted ashes, resulting in a higher theoretical value.

Table 13. Comparison of Theoretical and Measured $\delta^{18}\text{O}$ ratios for plant ash glasses

	Run 6 (1326)	Run 7 (1330)	Run 12 (1381)	Run 20 (1331)
Theoretical	11.6	10.5	10.4	10.7
Measured	10.0	10.2	9.7	9.8
std dev.	1.1	0.2	0.5	0.6

The average $\delta^{18}\text{O}$ value for all plant-ash glasses is 9.8‰. The average of the natron glasses is 9.7‰, and this value is within the experimental error for the plant ash glasses.

Although the two types of glasses are made with different ingredients their isotopic signatures end up being very similar. The data in this study suggest that the isotopic signatures of the alkalis are not different enough to be used to differentiate between the two types of glasses.

Early isotope work by Brill (1970) reported very high isotopic ratios for natron (~ 39‰). Such a high ratio compared to the relative low ratio for silica (~11‰), are expected to elevate the isotopic signatures of the natron glasses to a higher value. Recent isotope work by Silvestri et al. (2010) also reports $\delta^{18}\text{O}$ for Wadi Natrun natron to be around 40‰. However, both of the analyses of the mineral alkalis done in this study (WY trona and 326) were much lower (15.4‰ and 9.7‰ respectively). The isotopic measurements made by Brill (1970) and Silvestri (et al., 2010) analyzed all of the oxygen in the natron (oxygen in H_2O and CO_3^{-2}). Lower oxygen values may be due to low yields of the mineral alkalis in this study, a difference in analytical techniques, or a real difference in the samples.

The mineral alkalis were heated to 900°C to simulate the heating effect on the alkalis during the fritting stage. Table 11 reports the isotopic ratios for the mineral glasses from each step of the glass-making process. Heating of the trona/natron samples in the fritting stages resulted the isotope ratio to decrease by 40% in the case of the WY trona glass, and by 20% in the 326 (Wadi Natrun) glass. The isotope ratios of the final glasses (WY trona glass – 10.0‰; 326 glass 9.5‰) are lower than that of the Spruce Pine quartz (11.7‰) but are within the same range of error as the plant ash glasses.

CONCLUSIONS

This research was undertaken in hope of developing a compositional classification system for ancient glasses based on oxygen isotope ratios. The results of this study suggest that chemical characterization is still the most effective way to classify ancient glasses. Electron microprobe analysis is shown successful in characterizing glasses chemically. However, care should be taken when analyzing high-sodium glasses, as glasses of this type tend to be more susceptible to sodium migration and electron beam damage. The K_2O/MgO classification that has been used to differentiate between plant-ash type and natron-type glasses may not be able to successfully classify every glass artifact. Results of this study show the $MgO-K_2O$ contents of the glasses are clearly dependent on the *type of plant* used to flux the silica. The success of the K_2O/MgO classification is attributable to some uniformity on the selection of plant type used in the glass preparation.

Differentiating between the plant ash and mineral alkalis based on the $\delta^{18}O$ ratio of the glasses is not likely as all the experimental glasses have $\delta^{18}O$ values between 9.5 and 10.2‰. Analysis of the ^{18}O -content of the raw materials during each step of the glass-making process shows how heating can affect isotope ratios. Although the plants have very high $\delta^{18}O$ ratios before they are ashed, the majority of the oxygen (over 60%) is lost during the ashing and fritting stages. The mineral alkalis also show the same gradual loss in oxygen during the heating process. By the time the alkalis are fritted, their $\delta^{18}O$ values are within the same range and therefore produce glasses that have the same $\delta^{18}O$ values. Since the major contributor of the oxygen is the silica component, and the alkalis contribute such small amounts of oxygen, their

effect in the final $\delta^{18}\text{O}$ value is negligible. Alleged success in the use of oxygen isotopes to distinguish mineral and plant glasses (e.g. Silvestri et al. 2010) is probably due to differences in the oxygen isotope composition of the silica source.

Future research may find that oxygen isotopes may be more effective as a complementary technique. Henderson et al. (2005) used oxygen isotopes as a complement to Sr-isotopes and found that strontium was much more effective at creating two distinct fields of plant-ash and natron glasses. Oxygen isotopes may hold more promise in provenance work, perhaps when chemical analyses alone cannot discriminate between source origins or manufacturing centers.

REFERENCES

- Barkoudah, Y. and Henderson, J. (2006) Plant ashes from Syria and the Manufacture of Ancient Glass: Ethnographic and Scientific aspects, *Journal of Glass Studies*, v. 48, p. 297-321
- Brill, R. H. (1970) Lead and Oxygen Isotopes in ancient objects. *Philosophical Transactions of the Royal Society of London. Series A, Mathematical and Physical Sciences*, v. 269 p.143-164
- Brill, R.H. (1999) *Chemical analysis of early glasses*, 2 vols, New York: The Corning Museum of Glass
- Brill, R. H., Clayton, R. H., Mayeda, T. K., and Stapleton, C. P. (1999) Oxygen Isotope Analyses of Ancient Glasses. In (Ed. R. H. Brill) *Chemical Analyses of Early Glasses, Volume 1*. Corning, New York: The Corning Museum of Glass, p. 301-322
- Clayton, R. N., and Mayeda, T. K. (1963) the use of bromine pentafluoride in the extraction of oxygen from oxides and silicates for isotopic analysis. *Geochimica et Cosmochimica Acta*, v. 27, p.43-52
- Douglas, R.W. and Frank, S. (1972) *A History of Glass-making*. London: Whitefriars Press Ltd.
- Gehre and Strauch (2003) High-temperature elemental analysis and pyrolysis techniques for stable isotope analysis. *Rapid Communications in Mass Spectrometry*, v. 17, 1497-1503
- Henderson, J (1985) The raw materials of early glass production. *Oxford Journal of Archaeology*, v.4, p. 267-291
- Henderson, J. (2000a) *The science and archaeology of materials*, London and New York: Routledge Press
- Henderson J. (2000b) Chemical analysis of ancient Egyptian glass and its interpretations, in *Ancient Egyptian materials and technology* (eds. P.T. Nicholson and J. Shaw) Cambridge: Cambridge University Press, p. 206-224

Henderson, J. (2002) Tradition and experiment in 1st millennium AD glass production – the emergence of early Islamic glass technology in late antiquity, *Accounts of Chemical Research*, v. 35, p. 594-602

Henderson, J. (2013) *Ancient Glass: an interdisciplinary exploration*. London: Cambridge University Press

Henderson, J., Evans, J.A., Sloane, H.J., Leng, M.J., and Doherty, C. (2005) The use of oxygen, strontium and lead isotopes to provenance ancient glasses in the Middle East. *Journal of Archaeological Science*, v. 32, p. 655-673

Henderson, J. Evans, J. and Y. Barkoudah (2009) The roots of provenance: glass, plants and isotopes in the Islamic Middle East. *Antiquity*, v. 83, p. 414-429

Kim, D.S. and Hrma P. (1992) Foaming in Glass Melts Produced by Sodium Sulfate Decomposition under Ramp Heating Conditions. *Journal of the American Ceramic Society*, vol. 75, p. 2959-2963

Kracek, F.C. (1930) System $\text{SiO}_2\text{-}2\text{Na}_2\text{O}\cdot\text{SiO}_2$. *Journal of Physical Chemistry*, vol. 34, p. 1588

Leslie, K.A., Freestone, I.C., Lowry, D. and M. Thirlwell (2006) The provenance and technology of Near Eastern Glasses: oxygen isotopes by laser fluorination as a complement to strontium. *Archaeometry*, v. 48, p. 253-270

Lilyquist, C. and Brill, R. H. (1993) *Studies in Early Egyptian Glass*. New York: The Metropolitan Museum of Art.

Lilyquist, C. and Brill, R. H. (1996) A collaborative study of early glassmaking in Egypt c. 1500 BC. *Annales du 13e Congrès de l'Association Internationale pour l'Histoire du Verre*. Lochem, the Netherlands: AIHV, 1996, pp. 1-9.

Moorey, P. (1999) *Ancient Mesopotamian Materials and Industries: the Archaeological Evidence*. Winona Lake, IN: Eisenbrauns.

Oppenheim, A. L., Brill, R. H., Barag, D., and von Saldern, A. (1970) *Glass and Glassmaking in Ancient Mesopotamia: An Edition of the Cuneiform Texts Which Contain Instructions for*

Glassmakers with a Catalogue of Surviving Objects. Corning, New York: The Corning Museum of Glass.

Rehren, T. (2000) New aspects of ancient Egyptian glassmaking. *Journal of Glass Studies*, v. 42, p. 13-24

Sayre, E.V. and Smith, R.W. (1961) Compositional categories of ancient glass. *Science*, v.133, p.1824-1826

Sayre, E.V. and Smith, R.W. (1974) Analytical studies of ancient Egyptian glass, in *Recent advances in the science and technology of materials* (ed. A. Bishay), vol. 3, New York: Plenum Press, p. 47-70

Shahid, K. A., and Glasser, F. P., 1972, Phase equilibria in the glass-forming region of the system Na₂O-CaO-MgO-SiO₂, *Physics and Chemistry of Glasses*, v. 13, p. 27-42

Shortland, A. J. (2004) Evaporites of the Wadi Natrun: Seasonal and annual variation and its implication for ancient exploitation. *Archaeometry*, v. 46, p. 497-517

Shortland, A. J., and Tite, M. S. (2000) Raw materials of glass from Amarna and implications for the origins of Egyptian glass. *Archaeometry*, v. 42, p.141-151

Shortland, A., Schachner, L. Freestone, I., and M. Tite (2006) Natron as a flux in the early vitreous materials industry: sources, beginnings and reasons for decline. *Journal of Archaeological Science*, v. 33, p. 521-530

Shortland, A., Degryse, P., Walton, M., Greer, M., Lauwers, V., and L. Salou (2011) The Evaporitic Deposits of Lake Fazda (Wadi Natrun, Egypt) and their use in Roman glass production. *Archaeometry*, v.53, p. 916-929

Silvestri, A., Longinelli, A., Molin, G. (2010) $\delta^{18}\text{O}$ measurements of archaeological glass (Roman to Modern age) and raw materials: possible interpretation. *Journal of Archaeological Science*, v. 37 p. 549-560

Stapleton, C. P. (2003) Geochemical analysis of glass and glaze from Hasanlu, northwestern Iran: constraints on manufacturing technology. Unpublished Doctoral Thesis, University of Georgia.

Stapleton, C. P. and S. E. Swanson(2002) Chemical analyses of glass artifacts from Iron Age levels of Hasanlu, northwestern Iran, *Journal of Glass Technology*, v. 43C, pp. 151-157.

Tanimoto, S. (2007) Experimental study of Late Bronze Age glass-making practice. PhD Thesis, UCL Institute of Archaeology, University of London.

Tanimoto, S. and Rehren, T. (2008) Interactions between silicate and salt melts in LBA glass-making. *Journal of Archaeological Science*, v. 35, p. 2566-2573.

The Glassmakers of Herat (1979) [video recording] (dir., prod.) Elliott Erwitt
Corning Museum of Glass: Corning, NY

Tite, M.S., Shortland, A., Maniatis, Y., Kavoussanaki, D., S.A. Harris (2006) The composition of the soda-rich and mixed alkali plant ashes used in the production of glass. *Journal of Archaeological Science*, v.33, p. 1284-1292

Turner (1954) Studies of ancient glass and the glass-making process. Part V: Raw Materials and melting processes. *Journal of the Society of Glass Technology*, v. 40, p. 277-30

Valley, J., Kitchen, N., Kohn, M., Niendorf, C. and M. Spicuzza (1995) UWG-2, a garnet standard for oxygen isotope ratios: Strategies for high precision and accuracy with laser heating, *Geochimica et Cosmochimica Acta*, v. 59, p. 5223-5231

Zerwick, C. (1990) *A Short History of Glass*, Corning: The Corning Museum of Glass